2018-07-01

Automated Impact Response Sounding for Accelerated Concrete Bridge Deck Inspection

Jacob Lynn Larsen
Brigham Young University

Automated Impact Response Sounding for Accelerated Concrete Bridge Deck Inspection

Jacob Lynn Larsen

A thesis submitted to the faculty of
Brigham Young University
in partial fulfillment of the requirements for the degree of

Master of Science

Brian A. Mazzeo, Chair
W. Spencer Guthrie
Gregory Nordin

Department of Electrical and Computer Engineering

Brigham Young University

ABSTRACT

Automated Impact Response Sounding for Accelerated Concrete Bridge Deck Inspection

Jacob Lynn Larsen
Department of Electrical and Computer Engineering, BYU
Master of Science

Infrastructure deterioration is an international problem requiring significant attention. One particular manifestation of this deterioration is the occurrence of sub-surface cracking (delaminations) in reinforced concrete bridge decks. Of many techniques available for inspection, air-coupled impact-echo testing, or sounding, is a non-destructive evaluation technique to determine the presence and location of delaminations based upon the acoustic response of a bridge deck when struck by an impactor. In this work, two automated air-coupled impact-echo sounding devices were designed and constructed. Each device included fast and repeatable impactors, moving platforms for traveling across a bridge deck, microphones for air-coupled sensing, distance measurement instruments for keeping track of impact locations, and signal processing modules. First, a single-channel automated sounding device was constructed, followed by a multi-channel system that was designed and built from the findings of the single-channel apparatus. The multi-channel device performed a delamination inspection in the same manner as the single-channel device but could complete an inspection of an entire traffic lane in one pass. Each device was tested on at least one concrete bridge deck and the delamination maps produced by the devices were compared with maps generated from a traditional chain-drag sounding inspection. The comparison between the two inspection approaches yielded high correlations for bridge deck delamination percentages. Testing with the two devices was more than seven and thirty times faster, respectively, than typical manual sounding procedures. This work demonstrates a technological advance in which sounding can be performed in a manner that makes complete bridge deck scanning for delaminations rapid, safe, and practical.

Keywords: acoustic response, concrete bridge deck, delamination, impact-echo testing

ACKNOWLEDGEMENTS

I gratefully acknowledge the Utah Department of Transportation and U.S. Army Dugway Proving Ground for funding this research. BYU research assistants Jared Baxter, Joseph McElderry, Jeff Barton, Mandy Bitnoff, Danny Flannery, Jaren Knighton, Aaron Smith, Eric Sweat, Janelle Taysom, Tenli Waters, Lizzy Newbill, and David Young assisted with the field work and data processing. I'd like to thank Dr. Mazzeo and Dr. Guthrie for bringing me into this field as an undergraduate student with little experience. This research has shaped my career and I would never have been involved if not for them. I'd also like to thank the Electrical and Computer Engineering Department at Brigham Young University for the tuition assistance that was provided throughout my studies. Most importantly I'd like to express my deep gratitude for my wife, Jessica. She has spent countless hours taking care of our home and baby girl throughout this process and has been a huge support over the last 3 years. I wouldn't be where I am today without her.

TABLE OF CONTENTS

LIST OF TABLES

LIST OF FIGURES

1 INTRODUCTION

In 2016, 9.1% of bridges in the United States were considered structurally deficient [1]. While this is a serious problem for the United States, infrastructure deterioration is a global challenge. Trillions of dollars have been spent on the construction and maintenance of modern infrastructure and even more will be spent on efforts to maintain and repair these expensive and important investments. As has been documented in various media outlets, addressing infrastructure deterioration is a major challenge, involving technical, economic, and political considerations. Solutions to this problem require interdisciplinary work and expertise from many different fields. To address one aspect of this global challenge, this thesis reports on technological advances in civil infrastructure inspection by automation of an acoustic impact response technique that is applied specifically to reinforced concrete bridge decks.

1.1 Bridge Deck Deterioration

One of the primary causes of structural deficiency in bridges, especially in colder regions, is deterioration caused by the use of chloride-based deicing salts [2, 3]. The bridge deck, out of all the elements of the structure, suffers the most from these deicing salts. It is also the hardest part to inspect due to traffic. When the chloride ions in the deicing salts diffuse through concrete bridge decks, corrosion of the embedded reinforcing steel can result [2]. As the corrosion process leads to the formation of rust, the volume of the steel increases, causing an expansion of the concrete from within the deck that eventually leads to a subsurface crack called a

delamination [4]. Delaminations are indicative of rapidly progressing deterioration and require either repair or replacement of damaged sections. Locating these delaminations and quantifying their extent is important for selecting appropriate maintenance and rehabilitation strategies to minimize overall life-cycle costs of bridge decks.

1.2 Impact-Echo Testing and Sounding

In the 1980s, the National Institute of Standards and Technology pioneered the impact-echo technique to identify delaminations in concrete surfaces [5, 6]. This traditional impact-echo test involved the use of steel ball bearings for striking the concrete, and contact sensors (accelerometers) used for measuring the echo and propagation of the pressure waves within the concrete following an impact [7, 8, 9, 10]. Because these pressure waves propagate differently in delaminated concrete than intact concrete, a Fast Fourier Transform was typically performed on the recorded echo, and classifications of the material condition were made based on the frequency spectra of the response signal. More recently, air-coupled techniques have been employed to reduce the necessity of contacting the bridge deck surface to measure the impact responses [11, 12, 13, 14, 15, 16, 17, 18]. Air-coupled impact-echo measurements are performed using microphones suspended above the test surface and can produce results similar to those obtained using contact sensors. Instead of directly measuring the pressure waves that propagate within the concrete, the microphones capture leaky surface waves or, perhaps more imperfectly in the case of concrete, flexural modes of the concrete that transmit acoustic energy through the air. This method of detection works best for delaminations with a ratio of areal size to thickness greater than five [19]. When the areal size is significantly greater than the thickness of the delamination, the flexural modes dominate the acoustic response of the concrete, and the delamination can be heard more easily.

In practice, the most common method to detect delaminations in bridge decks is sounding [20]. During a sounding inspection, the inspector typically taps on the deck with a hammer or drags a chain across the surface of the deck to excite an acoustic response from the concrete. This acoustic response, or "echo," is used to differentiate between intact and delaminated areas. When the inspector hears a "hollow" sound, he or she marks the area as delaminated and draws the location of the delamination on a map. In general, the flexural modes over a delamination resonate with a dominant frequency between 1.0 and 3.5 kHz, while on intact concrete they resonate at a frequency around 10 kHz [11]. When an inspector performs a typical chain drag of a bridge deck, the "hollow" sound that indicates a delamination is related to this difference in frequency. This process is analogous to air-coupled impact-echo techniques in that the inspector excites these flexural modes with a chain or hammer (impactor) and interprets the acoustic response with their ear instead of a microphone. Although sounding has been performed for decades, it relies heavily on the inspector's expertise and may be negatively influenced by inspector fatigue and ambient noise. Furthermore, marking the detected delaminations is a very slow process, and mapping the locations and sizes of the delaminations is tedious and may introduce additional errors. Depending on the length of the bridge, some sounding inspections can require days or even weeks to complete. Additional work is often done back at the office to digitize the delamination maps and to calculate whatever relevant statistics may be needed to make rehabilitation decisions.

For these reasons, researchers have been devising more automated methods for sounding of bridge decks [21, 22, 23]. Tinkey and Olson [24] developed a device with contact accelerometers that measured the surface waves propagating through the bridge deck following an automated impact from a pneumatic framing nailer. This device worked well for performing

traditional impact-echo tests but was dependent on good mechanical coupling between the contact accelerometers and the bridge deck surface; debris on the surface of the bridge deck can adversely affect this coupling and result in inconsistent measurements [24]. A device developed by Popovics [25] demonstrated the utility of air-coupled sensors [26, 27], microphones suspended above the test surface, that altogether eliminated the need for mechanical coupling. While this device was also capable of continuous data collection, it relied on rolling impactors that generated undesirable noise especially on rough concrete surfaces [25]. Zhang et al. [28] addressed the issue of excitation by building a rolling cart with an automated impactor comprised of a stainless-steel bar with a ball-shaped head that was lifted and released by a flywheel at a speed that generated two impacts per second. This device provided reliable excitation but relied on a limited training data set for analysis of acoustic responses using artificial neural networks. More recently, Sun et al. [29] developed an improved chaining method for generating impacts using a ball-chain device. This device increased the signal-to-noise ratio of the recorded acoustic response compared to a standard chain and was also shown to be less sensitive to variable roughness of the concrete surface; however, the dragging speed affected both the impact energy and the spatial resolution. This research aims to build upon these technological advancements while also addressing some of their limitations.

1.3 Single-Channel Automated Sounding Device

The first objective of this research was to develop an automated air-coupled impact-echo or automated sounding device for mapping the occurrence of delamination in a concrete bridge deck from a continuously moving platform with a fast, repeatable excitation mechanism and associated algorithms for collecting and analyzing the acoustic data [30]. This was accomplished by constructing an automated mallet that could rapidly strike a bridge deck and record the

acoustic response of each impact with a microphone. The recorded response could then be processed for each impact, and a classification of delaminated or intact could be made based on the processed audio. Theoretically, this device could be moved to any location on a bridge deck, generate an impact with the automated mallet, and determine whether the concrete is delaminated or intact. This device was tested on a bridge deck in Clearfield, Utah and the constructed apparatus and results of the field test are presented in Chapter 2.

1.4 Multi-Channel Automated Sounding Device

The second objective of this work was to build upon the single-channel automated sounding device and expand it into a multi-channel system [31]. Apart from constructing a multi-channel system from a single-channel unit, significant improvements were made in regards to impact generation, acoustic response recording, and audio processing for delamination classification. The multi-channel system is able to test an entire traffic lane on a bridge deck in one pass, rather than making multiple passes per lane with just a single mallet unit. Once completed, this device was tested on a bridge in Clearfield, Utah (the same bridge that was tested with the single-channel device) as well as three bridge decks in Park City, Utah. The development of the device and the results of the field tests are presented in Chapter 3.

1.5 Publications Resulting from This Work

Chapters 2 and 3 are modified papers resulting from this research that have been submitted for publication as of the time that this thesis was created. Including those papers, the following peer-reviewed publications have resulted from this work:

1. B. A. Mazzeo, J. Larsen, J. McElderry, and W. S. Guthrie, "Rapid multichannel impact-echo scanning of concrete bridge decks from a continuously moving platform," AIP Conference Proceedings 1806, 080003, 2017.

2. W. S. Guthrie, J. Larsen, J. Baxter, B. A. Mazzeo, "Automated Air-Coupled Impact-Echo Testing of a Concrete Bridge Deck from a Continuously Moving Platform," *Under Review*.

3. J. Larsen, J. McElderry, W. S. Guthrie, B. A. Mazzeo, "Automated Sounding for Concrete Bridge Deck Inspection through a Multi-Channel, Continuously Moving Platform," *Under Review.*

1.6 Summary

Automation of the sounding process with these devices significantly decreases the standard bridge deck inspection time, eliminates the subjectivity associated with traditional sounding techniques, and increases the safety of the inspection process by substantially reducing the exposure of inspectors to live trafficking. Automation of traditional manual sounding procedures with devices like those developed in this work can save Departments of Transportation (DOT) significant amounts of time and money. Monitoring the structural integrity of the nation's bridges and execution of maintenance or rehabilitation can become more efficient by implementing modern technology into our bridge management systems.

2 SINGLE-CHANNEL AUTOMATED SOUNDING DEVICE

The scope for the first stage of this research included designing and building the new device, developing algorithms for processing the acoustic data, and determining a delamination detection threshold by comparing the results obtained using the new device with those obtained from traditional chain dragging in a field demonstration. The following sections provide a description of the automated sounding device and associated algorithms developed in this work, discussion of the results of the field demonstration, and conclusions and recommendations derived from the findings.

2.1 Apparatus Development

The apparatus developed in this research included an impactor unit, a moving platform, a microphone for air-coupled sensing, a distance measurement instrument (DMI), and signal processing modules. The impactor unit designed for bridge deck testing in this research included several individual elements as depicted in Figure 2-1. Based on previous work in which a softer impact material was shown to improve excitation of flexural modes in concrete by facilitating a longer contact time between the impactor and the concrete surface [32], a Musser M5 percussion mallet was selected for the present work due to its shaft length and flexibility as well as its mallet head size and composition. The mallet was actuated using a Pittman 19.5:1 gear-reduction motor, which was mounted to the back side of an aluminum plate for rotating a cam shaft

attached to the motor spindle. The cam shaft rotated in a clockwise direction, as viewed in Figure 2-1, to elevate the mallet head above the concrete surface. As the cam shaft released the mallet, which rotated about a pivot point, a spring mounted above the mallet shaft caused a sudden downward motion of the mallet head. The mallet head then impacted the concrete

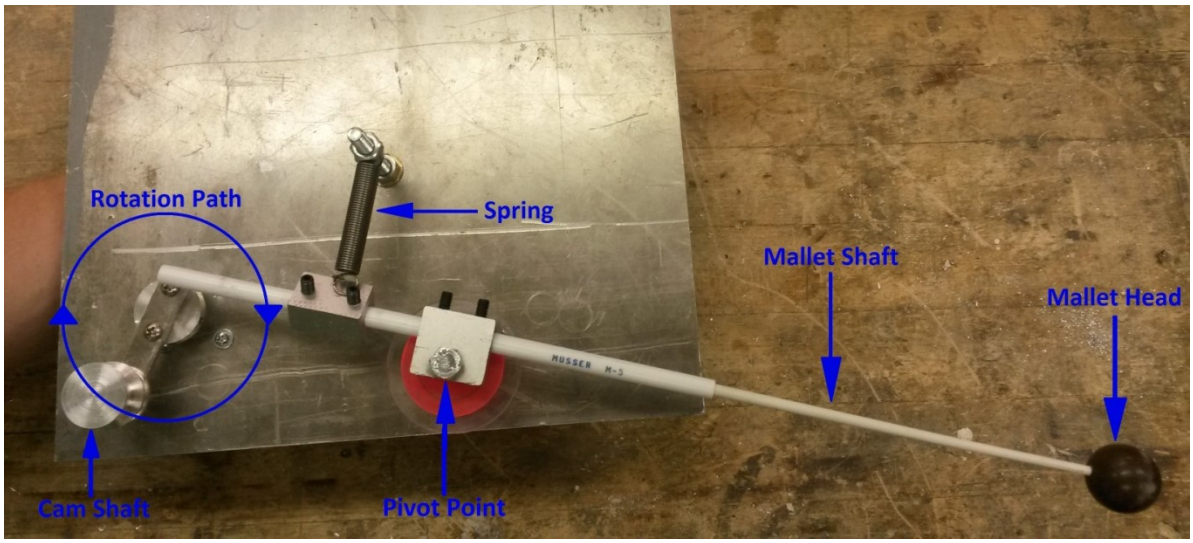

Figure 2-1. Mallet impactor unit.

surface. As the motor continued to rotate the cam shaft, consistent impacts were repeatedly generated independent of the speed of the moving platform. A high impact rate on the order of four impacts per second, which was twice as fast as that reported by Zhang et al. [28], was achieved using a Tektronix PS280 power supply set to approximately 20 volts.

The impactor was mounted within a moving platform, or cart, as illustrated in Figure 2-2. The cart was constructed of wooden panels lined with foam to acoustically isolate the impactor and other interior elements from ambient noise; this approach eliminated the need to account for such noise, which can require complex numerical methods [28]. As shown in Figure 2-3, the inner cavity of the cart was divided into two sub-cavities. One contained the mallet, which was

mounted to a side panel, while the other contained the microphone used for recording the acoustic response of the bridge deck during excitation. This cavity division limited the influence of the direct acoustic wave, generated by each impact, on the recording of the concrete vibration and thereby increased the signal clarity of the concrete response.

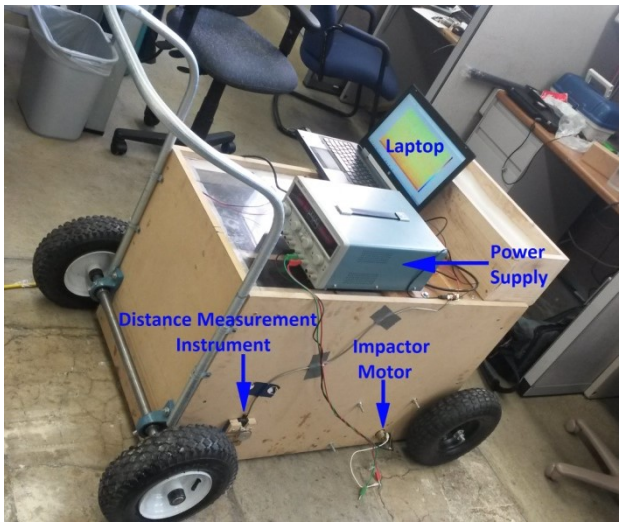

Figure 2-2. Automated sounding cart with power supply for impactor and laptop for post-processing and recording.

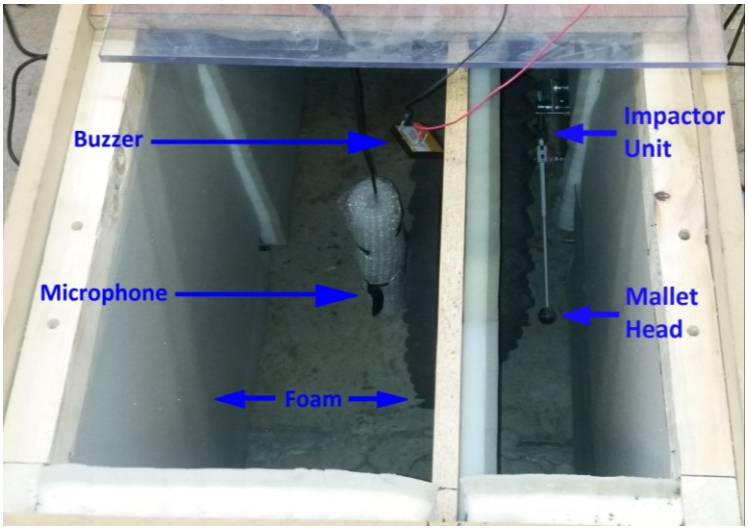

Figure 2-3. Interior of the automated sounding cart.

The cart was designed to be pushed by an operator across a bridge deck surface in multiple passes to automatically generate impacts and record the acoustic responses, and it was equipped with large pneumatic tires to ensure quiet, stable rolling across the bridge deck surface, even in the presence of debris.

A microelectrical-mechanical system (MEMS) Dodotronic ultrasonic microphone (Ultramic250k) with an effective frequency range of up to 125 kHz was chosen to accomplish the air-coupled recording of impacts. The microphone was placed inside a protective layer of plastic and suspended from the top of the cart directly across from the mallet head on the other side of the dividing panel. The microphone was positioned so that the diaphragm was about 50 mm above the concrete surface. Prior to recording the acoustic responses of the concrete under excitation, the microphone first recorded a tone generated by a buzzer, which was actuated by the operator to signal the start of a new pass. The recorded buzzer sound was used in post-processing of the data to locate the beginning of the pass in the audio record.

The cart was also instrumented with a DMI, as shown in Figure 2-2, to automatically record the traveled distance of the cart during testing. The distance was measured using a US Digital S1-500-250-NE-B-D rotation encoder that was connected to the rear axle of the cart with a tensioned rubber belt. The belt was guided through pulley wheels mounted on the rotation encoder and rear axle. As the cart moved across a deck surface, the rotation encoder produced electrical pulses that were counted by a Teensy 3.1 microcontroller used to interpret the data and deliver the information to an attached laptop.

A laptop was used for recording the microphone measurements, keeping track of distance traveled, and signal processing. Time stamps applied to the impact recordings and distance measurements were used to associate those two data sets using linear interpolation between

distance measurements. Impact events within the recording were identified at times when the audio level exceeded a defined threshold. Signal processing was then performed on the data corresponding to those times. As delaminations exhibit flexural vibrations that are lower in vibration frequency than those exhibited by intact concrete under excitation [11, 33], a Fourier transform was used for analyzing the frequency spectrum of the acoustic response to determine if the concrete was intact or delaminated. More specifically, the following algorithm was implemented in MATLAB. The acoustic waveform data had a representation in MATLAB that ranged from -1 to 1 with a standard deviation of approximately 0.03 for most runs. To find times when impacts occurred, time stamps were recorded when the signal deviated below its median value by a value of at least 0.1. At those locations in the acoustic waveform record, 6001 audio samples were then selected for further processing, representing about 24 ms of acoustic data. An additional constraint was enforced that impacts were required to be at least 0.12 seconds apart to ensure that single impacts were processed only once. The 6001 samples representing a single impact were downsampled by a factor of 10 and then the MATLAB periodogram power spectral density estimate with a rectangular window was computed using a 2048-point FFT. Bins 80 to 136, representing frequencies from 964 Hz to 1.65 kHz, were then summed to estimate the bandlimited acoustic energy (BAE) over this selected time period after the impact. These parameters were determined before comparison with the chaining data, however, these windows of frequency and time were chosen for identifying delaminations due to the high acoustic energy associated with them and are within the range of 0.5 to 5 kHz computed using semi-analytical equations of resonance frequencies for square delaminations having a depth of 20 to 80 mm and a width of 0.2 to 1.0 m [11]. Additionally, for the soft mallet impactor used in this study, this range appeared to adequately capture the acoustic signature of delaminations. This approach of

summing a broad range of spectral energy captures variations naturally present in the depth and extent of the delaminations on the deck.

2.2 Field Demonstration

After the apparatus was complete, a field demonstration was arranged on a concrete bridge deck in northern Utah. The bridge carried one lane of eastbound traffic and one lane of westbound traffic over several railroad tracks. With 11 spans, the bridge had a total length of 434 m, and the width of the bridge between the inside faces of the parapet walls was 8.7 m. The bridge was constructed in 1972 using uncoated reinforcing steel, or black bar, and a 25-mm-thick concrete overlay was placed in 1973. A nearly 10-mm-thick polymer surface treatment was applied to the bridge deck approximately 30 years later. With an original cover depth of 50 mm over the top mat of reinforcing steel, the average cover depth after these treatments was therefore 85 mm. At the time of the field demonstration in July 2014, the bridge was requiring weekly pothole maintenance on especially the span over the railroad tracks.

The field demonstration involved automated sounding with the new device and chaining. For testing, the deck was divided into sections in alphabetical order from A to M with increasing longitudinal distance from east to west. These 13 sections corresponded to nine deck spans and two long slab spans, one at each end of the bridge, with the slab spans being divided into two sections each. A grid with 3-m spacing in the longitudinal direction and 1.2-m spacing in the transverse direction was marked on the deck surface for spatial referencing.

Automated sounding was performed with the new device along each of 12 longitudinal lines spaced 0.6 m apart in the transverse direction, excluding only the center line due to the presence of traffic control equipment at that location during testing. The automated sounding device delivered approximately four impacts per second, and the operator moved the device

along the line at a target speed of about 0.6 m per second. Each pass along the length of the bridge required approximately 20 minutes, so that testing of the entire bridge deck was completed in about 4-man hours. As described previously, a series of algorithms were then used to process the data.

In the process of chaining the deck, the researchers recorded the occurrence of delamination along each of the same 12 longitudinal lines evaluated using automated sounding and also along the center line. The deck condition, delaminated or intact, was recorded at 0.3-m intervals along each line. Each pass along the length of the bridge required an average of nearly 2.5-man hours, which equated to more than 30-man hours for the entire bridge deck.

The results of the deck testing include maps showing the automated sounding data and chaining data, as presented in Figure 2-4 (not drawn to scale). For display purposes, a cubic interpolation function was used to generate values between the locations of the actual impacts and chaining measurements, which are indicated by black dots that appear as lines in the maps due to their close proximity to each other. In the automated sounding map, increasing BAE values indicate an increasing likelihood of delamination. In the chaining map, delamination indicator values of "0" and "1" indicate the absence and presence of delamination, respectively.

To determine if the span delamination percentages corresponded to observed differences in the acoustic impact data by the new device, and because universal standards for acoustic impact response are not yet established, a BAE threshold of 1.415×10^{-5} was selected to distinguish intact from delaminated concrete. This threshold was chosen because it resulted in the same delamination percentage for the entire bridge deck that was determined from chaining. As a means of evaluating its suitability across a broad range of delamination percentages, the same threshold of 1.415×10^{-5} was also used to compute the delamination percentage for each

individual test section. The results of automated sounding and chaining, presented in Table 2-1, were then compared using regression analysis as shown in Figure 2-5.

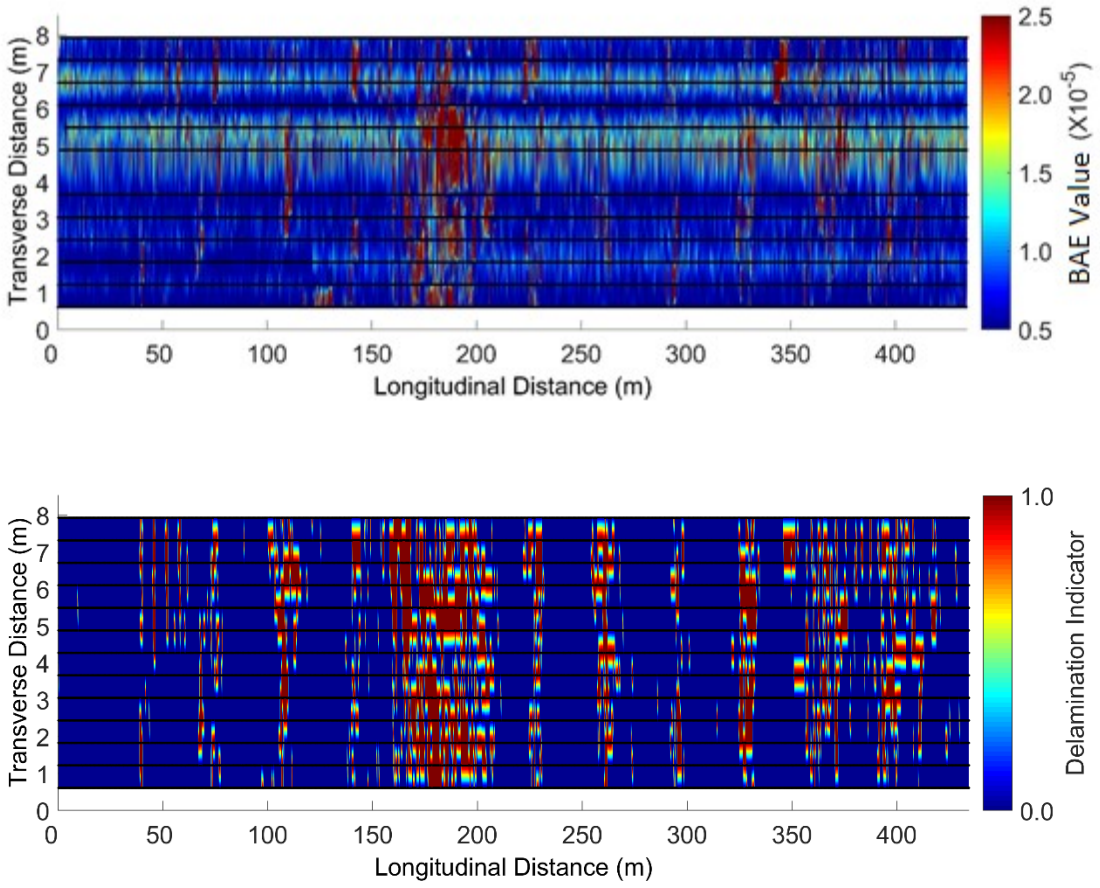

Figure 2-4. Automated sounding and chaining maps from the field demonstration. The Bandlimited Acoustic Energy is calculated using the methods outlined in the text.

2.3 Results and Discussion

The regression line shown in Figure 2-5 is characterized by a low *p*-value of 0.000 and a high coefficient of determination, or R^2 value, of 0.9623, which indicate a non-zero slope and an excellent fit of the data to the regression line, respectively.

Table 2-1. Summary of Deck Data by Test Section for Clearfield Field Demonstration

Test Section	Percentage of Deck Area (%) in Indicated Condition by Test Method			
	Automated Sounding		Chaining	
	Delaminated	Intact	Delaminated	Intact
A	6.5	93.5	0.1	99.9
B	10.0	90.0	9.5	90.5
C	9.2	90.8	7.6	92.4
D	11.7	88.3	10.1	89.9
E	16.1	83.9	24.6	75.4
F	42.7	57.3	56.2	43.8
G	15.5	84.5	13.9	86.1
H	11.0	89.0	11.1	88.9
I	11.1	88.9	8.5	91.5
J	12.2	87.8	9.7	90.3
K	17.1	82.9	16.7	83.3
L	19.8	80.2	20.9	79.1
M	12.6	87.4	12.0	88.0
Average	15.0	85.0	15.0	85.0

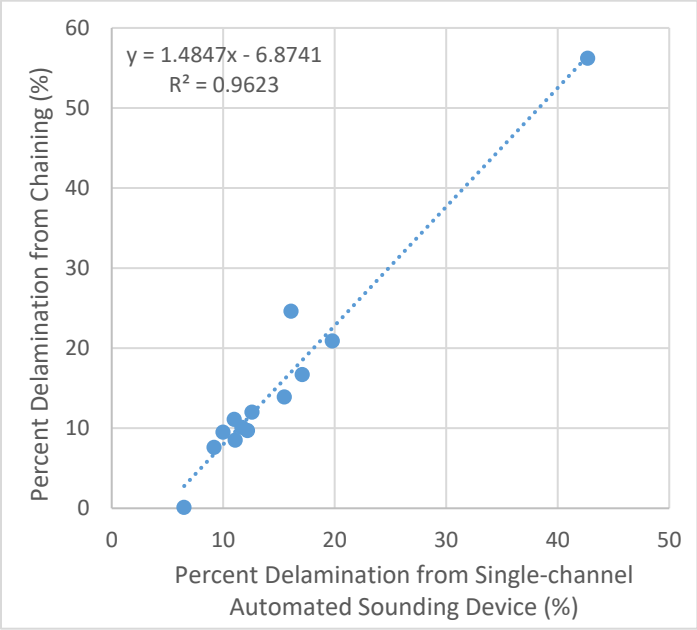

Figure 2-5. Regression analysis of automated sounding and chaining data.

Although the deviation of the regression line from the line of equality in Figure 2-5 suggests that some bias may exist in the automated sounding testing approach used in this work, the percentage of the deck area determined to be delaminated using automated sounding is within 3 percentage points of that determined to be delaminated using chaining for 10 of the 13 test sections (test sections B, C, D, G, H, I, J, K, L, and M), which generally exhibit delamination percentages ranging from 7 to 21 percent. Among the remaining three test sections, test section A is characterized as having the lowest delamination percentage at less than 1 percent, while test sections E and F are characterized as having the highest delamination percentages at greater than 24 percent according to the chaining results; the percentage of the deck area determined to be delaminated using automated sounding is approximately 6 percentage points higher for test section A and up to 14 percentage points lower for test sections E and F than the corresponding percentages of the deck area determined to be delaminated using chaining. Such variations between the results of the automated sounding and chaining tests may be partially attributed to possible tracking differences along each of the longitudinal lines, exclusion of the center line during the automated sounding tests, and/or minor distance measurement differences that may have occurred between the two approaches.

2.4 Conclusions

The primary accomplishment of this part of the research is the development of a single-channel automated sounding device for mapping the occurrence of delamination in a concrete bridge deck from a continuously moving platform with a fast, repeatable excitation mechanism and unsupervised algorithms for collecting and analyzing the acoustic data. The apparatus included an impactor unit, a moving platform, a microphone for air-coupled sensing, a DMI, and signal processing modules. Field testing of a concrete bridge deck with a length and width of

434 m and 8.7 m, respectively, required about 4-man hours using the new device compared to more than 30-man hours required for chaining; therefore, testing with the new device was more than seven times faster than chaining. A comparison of the automated sounding data with the chaining data yielded a BAE detection threshold of 1.415×10^{-5}, and the resulting percentage of the deck area determined to be delaminated using automated sounding was within 3 percentage points of that determined to be delaminated using chaining for 10 of the 13 test sections into which the deck was divided. These test sections generally exhibited delamination percentages ranging from 7 to 21 percent, demonstrating the utility of the new automated sounding testing for evaluating concrete bridge decks with various amounts of delamination.

While the automated sounding device developed in this research incorporated only a single channel, the apparatus could be readily expanded to a multi-channel system that would allow even faster bridge deck testing. The development of such a device is detailed in the next chapter. Nonetheless, given the typical threshold values for delamination percentages utilized for bridge management, the data suggest that the new automated sounding device could be used to generate results that would lead to similar maintenance and rehabilitation strategies as those that would be recommended based on the results of chain dragging. Additional work to optimize the use of the new acoustic data analysis algorithms presented in this work may provide even better results; specifically, a larger frequency summing window may provide greater detection capability.

3 MULTI-CHANNEL AUTOMATED SOUNDING DEVICE

The second stage of this research included the design and construction of the new multi-channel device, improvement of the algorithms used for processing the acoustic data with the single-channel device, and the determination of a delamination detection threshold by comparing the results obtained using the multi-channel device with those obtained from traditional chain dragging in field demonstrations. The following sections provide a description of the multi-channel automated sounding device and associated algorithms used for processing, discussion of the results of the field demonstrations, and conclusions and recommendations derived from the findings.

3.1 Apparatus Development

The multi-channel automated sounding device includes seven replicated impactor and recording units, a moving trailer platform, a distance measurement instrument (DMI), and signal processing modules. The impactor unit from the single-channel device was improved upon for the multi-channel device and comprises several individual elements as depicted in Figure 3-1. As mentioned in Chapter 2, impact materials that are softer than steel have been shown to improve excitation of flexural modes in concrete [32] due to the increased contact time they exhibit during an impact [10]. Because of this, the mallets were constructed using a 38.1-cm polypropylene shaft (UL 94HB) and a 2.54-cm-diameter brass head (Liberty Brass BAL132). The polypropylene shaft is able to flex as the brass head contacts the surface, which increases the

contact time of the brass head and delays the recoil, similar to the percussion mallet (Musser M5) used on the single-channel device [30]. The mallets are actuated using a 19.5:1 gear-reduction motor (Pittman GM9236S020-R1), which is mounted to the back side of a 0.64-cm-thick aluminum plate for rotating a 3D printed polylactide (PLA) cam attached to the motor spindle. The cam rotates in a clockwise direction to elevate the mallet head above the concrete surface. As the cam releases the mallet, which rotates about a fulcrum (Fastenal 0120659), a spring (Century Spring 5984) mounted above the mallet shaft pulls the end of the mallet upward and causes the mallet head to accelerate towards and strike the surface. The motor rotates once every 1.32 s and repeatedly generates impacts at this rate as the motor rotates.

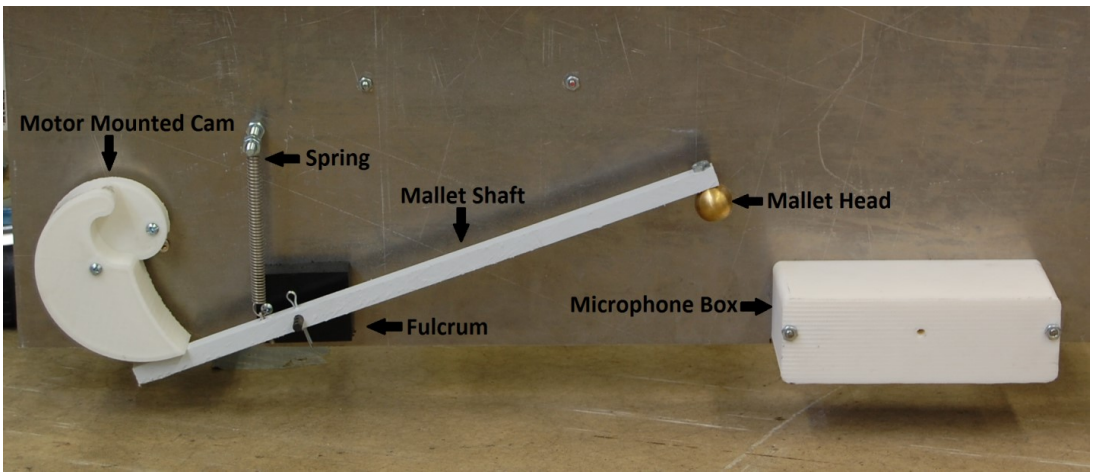

Figure 3-1. Mallet impactor unit showing basic arrangement of components.

Each mallet is assigned its own Freescale FRDM-K64F development board (Digikey FRDM-K64F-ND), attached to which is a daughter board with custom circuitry designed to drive the motor and record the acoustic responses captured by the microphones. The entire control board is shown in Figure 3-2. Electret condenser microphones (CUI Inc. CMB-6544PF) were used for the air-coupled recording of impacts. Each microphone was connected to a simple

analog amplifier circuit on the custom microcontroller shield and placed inside a custom box that is 3D printed from a Polylactic Acid (PLA) material. This box is mounted to the aluminum mallet unit plate 2.54 cm from the mallet head as shown in Figure 3-1. The microphone is positioned so that the diaphragm is about 2.54 cm above the concrete surface.

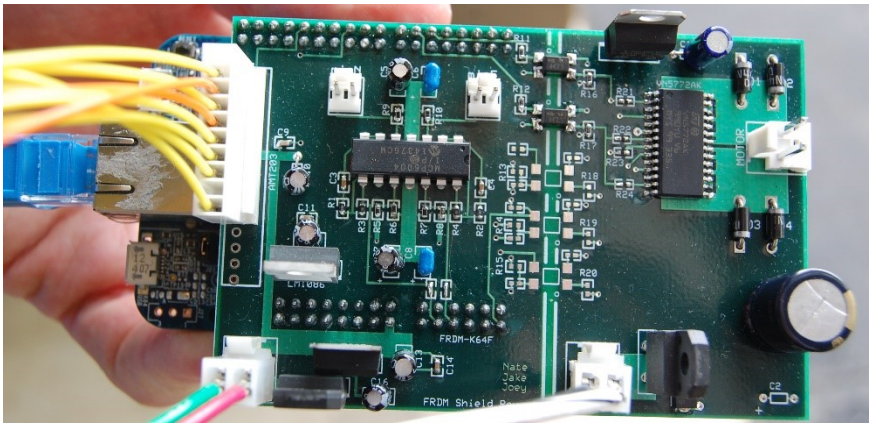

Figure 3-2. Custom motor control and microphone amplification daughter board mounted on a FRDM-K64F development board, with the ethernet cable and wires to the power source, microphones, and rotation encoder shown.

Seven impactor units are mounted to a moving trailer platform, as illustrated in Figures 3-3 and 3-4. The trailer is constructed of 5.08-cm x 5.08-cm square steel tubing with 3.18-mm-thick walls and hinges to allow for folding and unfolding of the trailer. Each mallet is placed on the trailer 61.0 cm from the adjacent mallets, which results in a total trailer width of 3.76 m, or approximately the width of a standard traffic lane, when the trailer is unfolded. The two wing sections of the trailer can be folded on top of the middle trailer section to reduce the trailer width to 1.98 m for stowing and transport. The hitch section of the trailer is built with a double hinge configuration to accommodate variations in truck hitch height and to allow the trailer to move up and down with the bridge deck as bumps, potholes, or other variations of concrete curvature are encountered along the traveled path on the bridge deck. The trailer is equipped with 25.4-cm-

diameter pneumatic caster wheels (Harbor Freight 60249 and 61450) to ensure stable rolling across the bridge deck surface. As shown in Figure 3-3, the entire folded trailer can be loaded on and off the hitch of a truck by using a winch (Harbor Freight 61257) with a 1587-kg weight capacity, which makes travel and deployment of the trailer very efficient. Upon arrival at a bridge site, the trailer is winched down and unfolded to scan one lane at a time, as displayed in Figures 3-3 and 3-4. After an inspection is finished, the trailer is folded and winched up onto the hitch for immediate departure.

Figure 3-3. Photograph sequence showing deployment of the trailer for testing of a bridge deck, with lowering and unfolding of the apparatus requiring less than one minute.

Figure 3-4. Unfolded 3.76 m trailer ready for scanning a bridge lane.

Figure 3-5 shows the DMI mounted to the back of the trailer. The DMI consists of two 25.4-cm-diameter rubber tires (Harbor Freight 90051) mounted to a fixed 2.54-cm steel axle, together with a rotation encoder (CUI Inc. AMT203-V) that measures the rotation of the wheels as they roll across the bridge deck. A rubber belt is stretched across two pulleys, one attached to the axle and one attached to the rotation encoder, which ties the rotation of the encoder to the rotation of the axle. The number of rotation encoder ticks is counted for a single rotation of the DMI wheels, and the number of ticks per meter is computed using the circumference of the wheel, which enables assignment of a specific longitudinal position for each impact event with reference to a specific starting position on the bridge deck. Two light detection and ranging (LiDAR) units (PulsedLight LiDAR Lite V2) are also mounted to the DMI to measure the trailer distance from each parapet wall at all times during the inspection. The DMI and LIDAR measurements, which effectively provide x and y coordinates, respectively, for each impact with reference to a designated origin on the bridge deck, are recorded by another FRDM-K64F development board. Compared to other global positioning schemes that could have been used, the strategy utilized in this research enables more accurate relative positioning, on the order of 1 cm, during bridge deck testing without needing a static reference base station.

A connected laptop running a custom controller written in Python is used for controlling the impactor units, receiving and storing the impact audio recordings and position information, and signal processing. All impact audio recordings as well as DMI and LiDAR measurements are sent to the laptop over a Transmission Control Protocol (TCP) ethernet network from the individual impactor units and DMI modules used for data acquisition. Distance measurements are assigned to individual impacts based on recorded time stamps that are controlled by a common clock on the laptop.

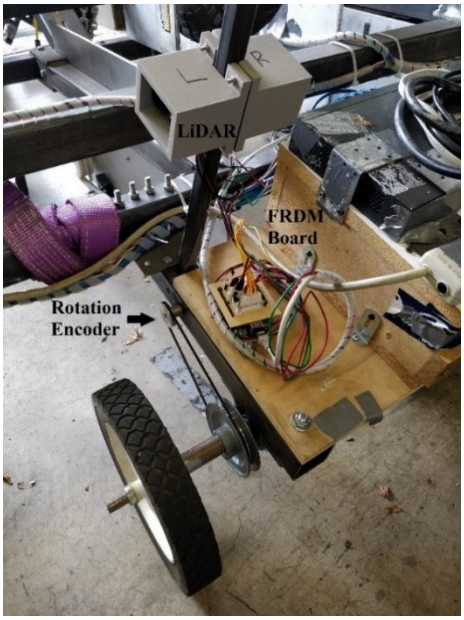

Figure 3-5. DMI and LiDAR units used for measuring the trailer position during bridge deck scanning.

During bridge deck scanning, only the audio shortly before, during, and immediately after an impact is recorded. The audio was recorded at a sampling frequency of 44.1 kHz with a recording time of 0.19 seconds per impact. The execution and recording of the impacts is carried out sequentially so that no two impactor units execute an impact at the same time. This arrangement ensures that each microphone records only the impacts that are generated by the impactor unit to which the microphone is connected. Each impactor unit is configured to generate an impact every 0.19 seconds, meaning that all the impactor units generate one impact each during a 1.32-second time period. In practice, the trailer travels at about 0.3 meters per second so that each impactor unit executes an impact every 30 to 60 cm in the travel direction along the bridge deck.

A series of computer algorithms is used to determine the presence of delamination on the deck. Specifically, the Bandlimited Acoustic Energy (BAE) is determined for each impact as the sum of spectrogram coefficients for the recorded audio over a window covering 1 kHz to 4 kHz

during the 30 milliseconds after the impact. This same delamination classifier was used with the single-channel device but with different frequency and time values used for the summing window. On this device, the frequency window was widened so that a broader range of frequencies was captured at which delaminations commonly resonate. Overall, these parameters were selected for identifying delaminations due to the high acoustic energy associated with them [11]. The spectrogram coefficients were generated with a hamming window and a 2048-point FFT. Figure 3-6 presents example spectrograms that display the frequency responses of two impacts generated by the automated sounding device, one on intact concrete and one on delaminated concrete. The vertical columns in the spectrograms represent the impacts and the resulting bounce of the mallet after the original impact. The red box indicates the window over which the spectrogram coefficients are summed to generate a BAE value for each impact. As evidenced by the differing intensities of the yellow regions inside the red box, the bandlimited, low-frequency acoustic energy associated with the impact on the delamination is much higher than that associated with the impact on intact concrete. This result indicates that the use of the summation of spectrogram coefficients from 1 kHz to 4 kHz is a potentially useful means of differentiating between intact and delaminated concrete. The data analysis process for the BAE and position measurements for each impact is presented in Figure 3-7.

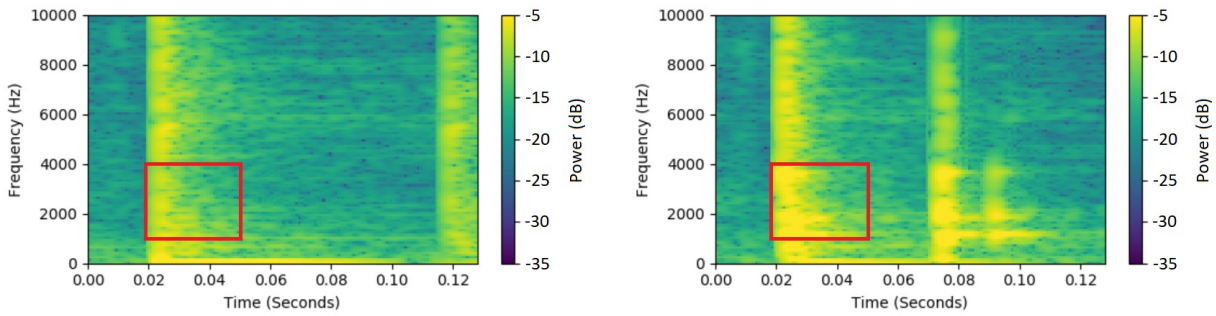

Figure 3-6. Spectrograms of impacts on an intact (left) and delaminated (right) section of concrete, in which the red box indicates the window where the spectrogram coefficients are summed to produce the BAE value.

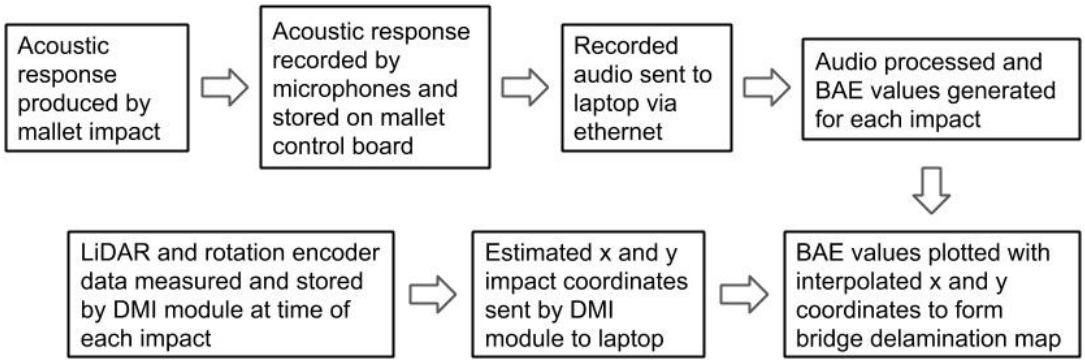

Figure 3-7. Data analysis process for generating a delamination map from measurements of BAE and position.

3.2 Field Demonstrations

The field demonstrations for the multi-channel automated sounding device were carried out in Clearfield, Utah (June 2015) and Park City, Utah (June 2016). Between the two field demonstrations, modifications were made to the trailer to improve the inspection process. These modifications are discussed in detail later on. The purposes of the field demonstrations were to determine an appropriate threshold BAE value for distinguishing between intact and delaminated concrete and to compare the spatial distributions of delaminations detected using the automated sounding trailer with those detected using chain dragging. The first field demonstration was arranged on the same bridge deck that was tested with the single-channel automated sounding device [30]. The total length of the bridge deck was 434 m, and the width of the bridge between the inside faces of the parapet walls was 8.7 m.

For testing, two passes, one for each lane, were made over the bridge deck using the automated sounding trailer. Each pass was performed with the edge of the trailer located about 0.3 m from the nearest parapet wall. The 0.6-meter-wide section in the middle of the bridge for the lane dividing line was excluded from the passes made by the trailer due to the presence of

traffic cones. Testing of the entire bridge deck was completed in about 1 hour. The chaining inspection performed in July 2014 required more than 30-man hours.

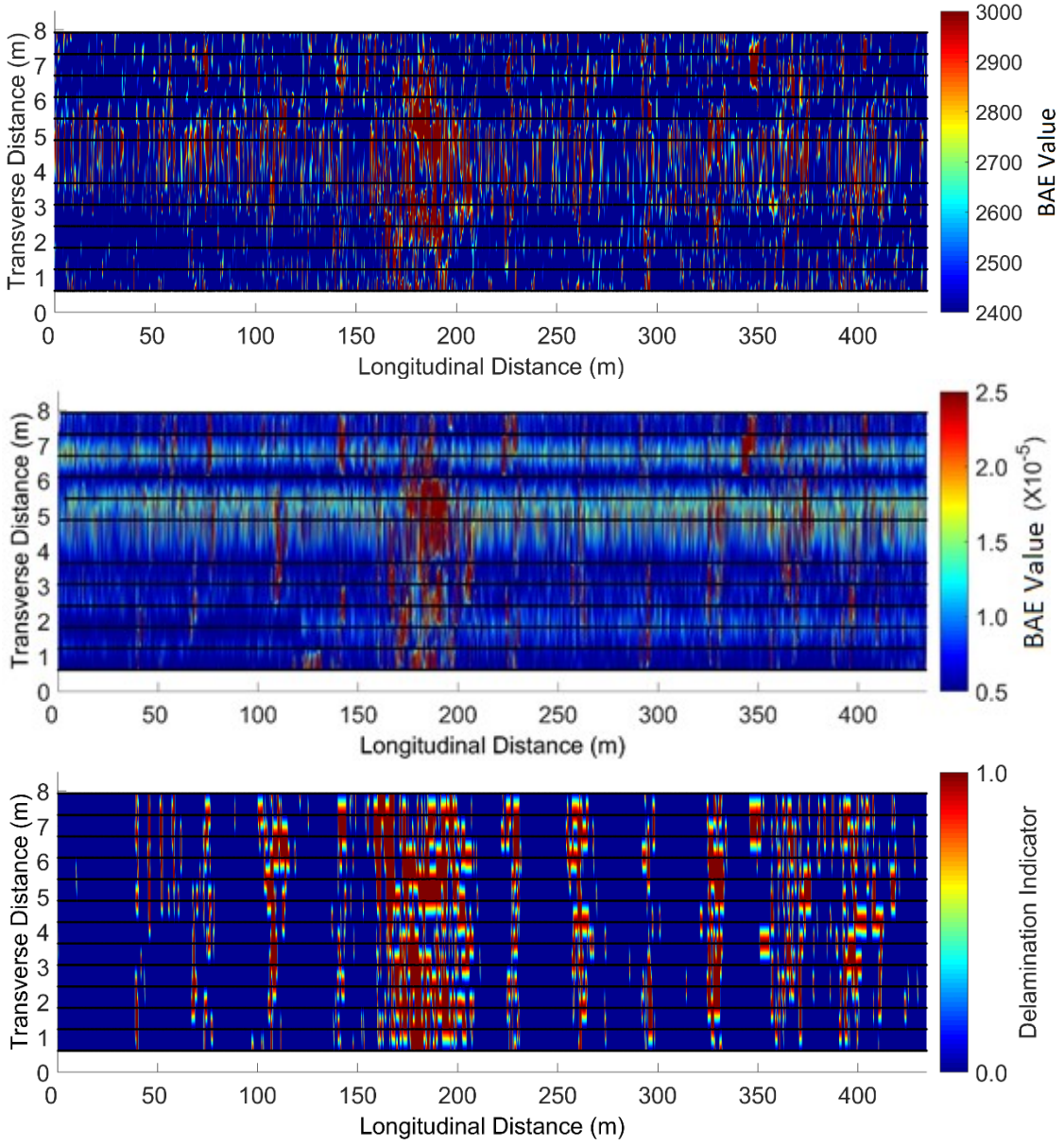

Figure 3-8. Multi-channel automated sounding trailer (top), single-mallet automated sounding device not reported in this work (middle), and chaining (bottom) maps from the field demonstration.

Maps generated from the multi-channel automated sounding trailer data, the single-mallet automated sounding device data, and manual chaining data, are shown in Figure 3-8 (not drawn to scale). The maps for the single-channel device data and chaining data are the same maps that were presented in Chapter 2 and are included here for comparison to the multi-channel device. For display and analysis purposes, a linear interpolation function was used to generate values between the locations of the impacts and chaining measurements, which are indicated by black dots appearing as lines in the maps due to their close proximity to each other. In the automated sounding maps, increasing BAE values indicate an increasing probability of delamination. In the chaining map, delamination indicator values of "0" and "1" indicate the absence and presence of delamination, respectively.

Table 3-1. Summary of Deck Data by Test Section for Clearfield Field Demonstration

Test Section	Percentage of Deck Area (%) in Indicated Condition by Test Method			
	Automated Sounding		Chaining	
	Delaminated	Intact	Delaminated	Intact
A	7.9	92.1	0.1	99.9
B	9.2	90.8	9.5	90.5
C	10.4	89.6	7.6	92.4
D	13.4	86.6	10.1	89.9
E	18.1	81.9	24.6	75.4
F	40.0	60.0	56.2	43.8
G	15.3	84.7	13.9	86.1
H	11.3	88.7	11.1	88.9
I	9.9	90.1	8.5	91.5
J	14.7	85.3	9.7	90.3
K	18.1	81.9	16.7	83.3
L	17.8	82.2	20.9	79.1
M	13.6	86.4	12.0	88.0
Total %	15.3	84.7	15.0	85.0

An important goal of this work was to determine if different delaminated and intact regions could be distinguished reliably on a large deck by treating different sections of the deck independently and then estimating their delamination percentages. Their individual delamination percentages could then be used as a test for reliability of the method. To accomplish this, a BAE threshold was selected that resulted in nearly the same total amount of delamination for the entire bridge deck that was determined from chaining. This threshold, a BAE value of 2700, was then used to compute the extent of delamination for each test section. The same 13 test sections (A through M) used for analysis in our Chapter 2 are used here. Delamination percentages calculated from both the automated sounding and chaining inspections for each test section are presented in Table 3-1.

After the first field demonstration in Clearfield, Utah, the microphones on each mallet were changed to a Knowles digital MEMS microphone (SPH0641LU4H-1). This was done because the electret microphones broke easily and required custom power circuitry. Other advantages to using MEMS microphones include small physical size, broad frequency bandwidth, and high SNR [34]. Minor changes to the mallet control and audio processing code were also made to accommodate this change in microphone. Specifically, the sampling frequency was set to 3.75 MHz and the recording time for each impact was kept at 0.19 seconds. The output of the microphone is a pulse-density modulated (PDM) signal which needed to be converted to an analog audio signal before processing. In a PDM signal, the amplitude of the wave is represented by the average pulse amplitude over time. Applying a low-pass filter to the PDM signal essentially averages these pulses and returns an analog amplitude. To do this, a 2nd order Butterworth filter was used with a cutoff frequency of 20 kHz. The analog signal was then

processed in the same way as was explained previously and a BAE value was generated for each impact.

The second set of field tests with the automated sounding trailer was performed on three bridges along U.S. Route 40 in Park City, Utah, in June 2016. The bridges, which had bare concrete decks constructed using epoxy-coated rebar, were tested with the automated sounding trailer and also inspected via manual chain dragging during the same night. The bridges were all 27 years old, located within 1.6 km of each other, and subject to the same climate and annual average daily traffic. At the time of testing, the National Bridge Inventory ratings were 6, 7, and 6 for the first, second, and third bridge decks, respectively. Each of these bridges carried two lanes of traffic, each heading in the same direction. Each of the two lanes on each bridge deck was tested twice, with the second test in each lane occurring at a target distance of 30.5 cm farther away from the parapet wall than the first test. This approach effectively doubled the resolution of the collected data by evaluating points on a 30.5-cm interval in the transverse direction rather than the fixed 61.0-cm spacing set by the mallet positions on the trailer.

Figures 3-9 and 3-10 present the resulting maps for the multi-mallet automated sounding trailer and chaining tests for two of the bridge decks. The third bridge experienced extensive delamination and the chain drag test was not completed due to the large amount of time it would have required to perform accurately; indeed, a visual inspection indicated that some delaminations had progressed to potholes on that deck, as evidenced by exposed rebar in some locations. Figure 3-11 presents the delamination map that was produced by the multi-channel device, but no comparison with a chain drag test is made for this bridge. The solid black lines in the automated sounding maps represent the parapet walls and joints indicating the beginning and end of the bridge deck. Because the microphones were changed between the first and second

field demonstrations, a new BAE threshold needed to be selected for the map production and delamination percentage calculations. The selection of this threshold was done in the same manner as was done in the first field demonstration. Delamination percentages were calculated from the chaining data and a BAE threshold was set for the automated sounding trailer data so that the estimated delamination percentage for the first bridge matched that of the first chaining inspection. This BAE threshold, 225000, was also used for the map production and delamination percentage calculations for the second and third bridges. The blue in the maps indicates the area that was classified as intact by the automated sounding device, while the red areas are classified as delaminations. After the selection of a BAE threshold, the first and second bridges were divided into five sections, with boundaries indicated by dashed lines in Figures 3-9 and 3-10. To enable a comparison of the spatial distributions of delaminations detected using the automated sounding trailer with those detected using chain dragging, delamination percentages were then computed for each section as shown in Tables 3-2 and 3-3.

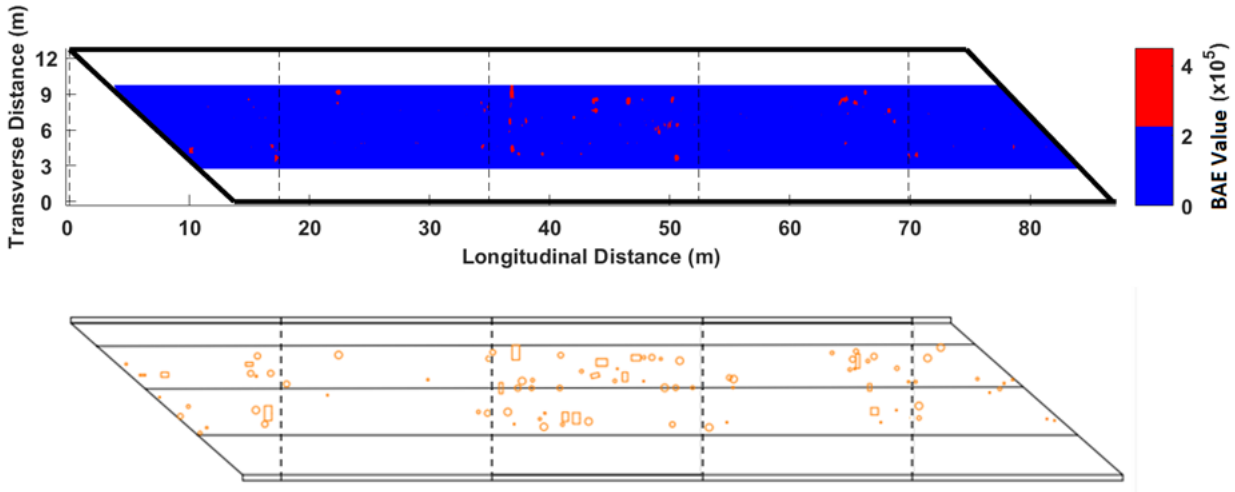

Figure 3-9. Maps for the automated sounding (top) and chaining data (bottom) from the first bridge.

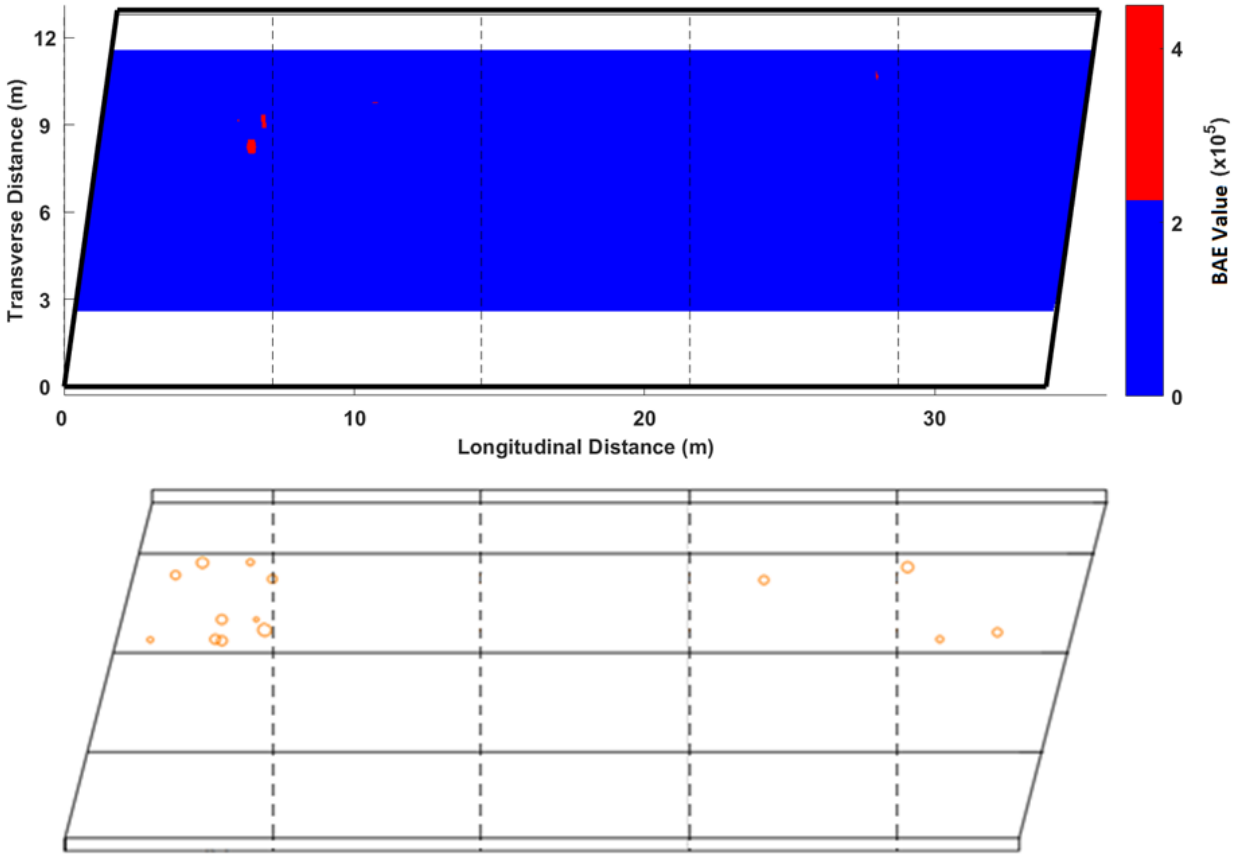

Figure 3-11. Maps for the automated sounding (top) and chaining data (bottom) from the second bridge.

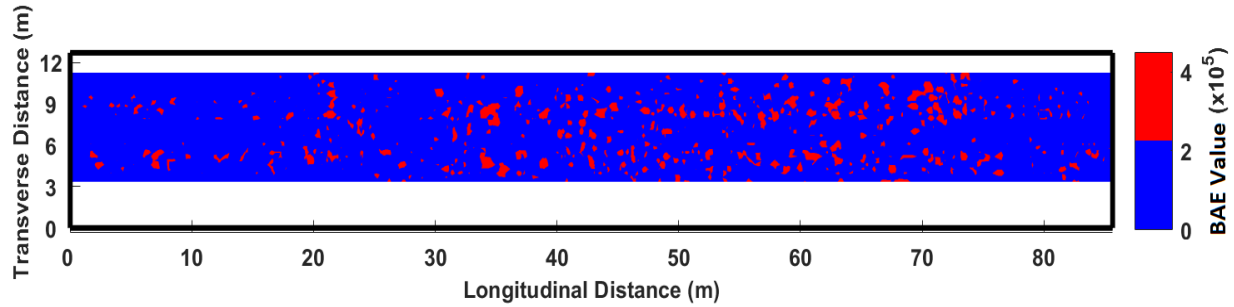

Figure 3-10. Map for the automated sounding data from the third bridge. This bridge experienced extensive delamination and a chain drag inspection was not performed.

Table 3-2. Summary of Deck Data by Test Section for second Field Demonstration Bridge 1

Test Section	Percentage of Deck Area (%) in Indicated Condition by Test Method			
	Automated Sounding		Chaining	
	Delaminated	Intact	Delaminated	Intact
1	1.22	98.78	2.13	97.87
2	0.85	99.15	0.46	99.54
3	3.21	96.79	3.22	96.78
4	1.47	98.53	1.20	98.80
5	1.15	98.85	0.97	99.03
Total %	1.63	98.37	1.61	98.39

Table 3-3. Summary of Deck Data by Test Section for second Field Demonstration Bridge 2

Test Section	Percentage of Deck Area (%) in Indicated Condition by Test Method			
	Automated Sounding		Chaining	
	Delaminated	Intact	Delaminated	Intact
1	0.37	99.63	1.10	98.90
2	0.18	99.82	0.02	99.98
3	0.00	100.00	0.00	100.00
4	0.06	99.94	0.08	99.92
5	0.00	100.00	0.35	99.65
Total %	0.13	99.87	0.27	99.73

3.3 Results and Discussion

The results of the automated sounding and chaining inspections for the first field demonstration in Clearfield, Utah, presented in Table 3-1, were then compared using regression analysis as shown in Figure 3-12. With an R^2 value of 0.9558, the calculated delamination percentages from the automated sounding and chaining inspections for each bridge section correlate well. This means that the device (with the selected BAE threshold) performed relatively well on each of the sections of the bridge. The maps in Figure 3-8 indicate that the

main areas of delamination found by the chaining inspection were also found by the automated sounding device. The main difference between the two inspection methods is the required time for completion. The automated sounding device was able to complete the deck inspection roughly 30 times faster than the chain drag inspection, not including the manual entering of chain drag information at the office, whereas for the automated methods the data processing time was negligible. Another important benefit of the automated sounding device is its ability to deliver a more consistent type of impact across the bridge deck than a manual chain drag or hammer sound. Delivering the same type of impact at every testing location is important for conducting a proper inspection and cannot be controlled when performing these tests manually. It is also important to note the improvement of the generated maps from the single-mallet device to the multi-mallet device. The use of brass impactors rather than plastic provided a less noisy output and a map that more clearly correlates with the map produced from chaining. This is likely due to the brass head wearing down at a much slower rate than did the plastic mallet with the single-mallet device.

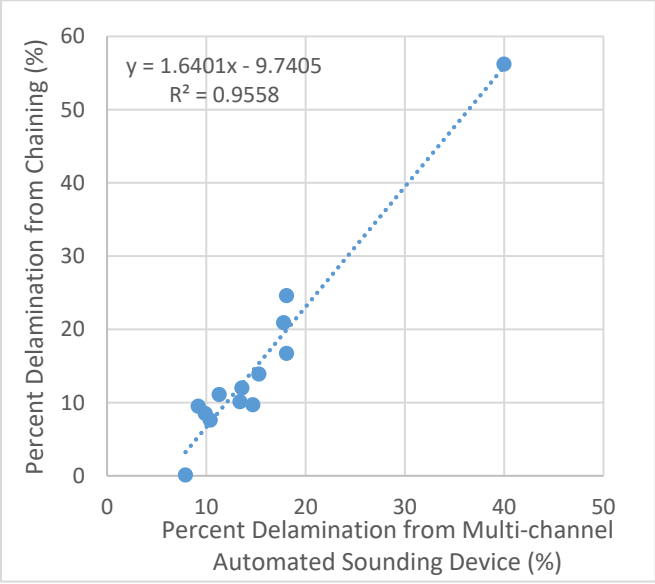

Figure 3-12. Regression analysis of automated sounding and chaining data for first field demonstration.

Table 3-4 presents a comparison of the delamination percentages returned by both the single-channel and multi-channel automated sounding devices for the first field demonstration in Clearfield, Utah. Figure 3-13 shows the regression analysis performed on this data set, which has an R^2 value of 0.9761. The delamination percentages returned by the single-channel and multi-channel devices are highly correlated, suggesting the success in replicating a single-channel device into a multi-channel system. When compared against the results of the chain-drag inspection, both single-channel and multi-channel devices differed most in delamination percentage on test sections A, E, and F. However, when comparing the two automated sounding devices with each other, these test sections match up well.

Table 3-4. Summary of Deck Data by Test Section from Two Sounding Devices for Clearfield Field Demonstration

Test Section	Percentage of Deck Area (%) in Indicated Condition by Test Method			
	Automated Multichannel Sounding Testing		Automated Single Channel Sounding Testing	
	Delaminated	Intact	Delaminated	Intact
A	7.9	92.1	6.5	93.5
B	9.2	90.8	10.0	90.0
C	10.4	89.6	9.2	90.8
D	13.4	86.6	11.7	88.3
E	18.1	81.9	16.1	83.9
F	40.0	60.0	42.7	57.3
G	15.3	84.7	15.5	84.5
H	11.3	88.7	11.0	89.0
I	9.9	90.1	11.1	88.9
J	14.7	85.3	12.2	87.8
K	18.1	81.9	17.1	82.9
L	17.8	82.2	19.8	80.2
M	13.6	86.4	12.6	87.4
Total %	15.3	84.7	15.0	85.0

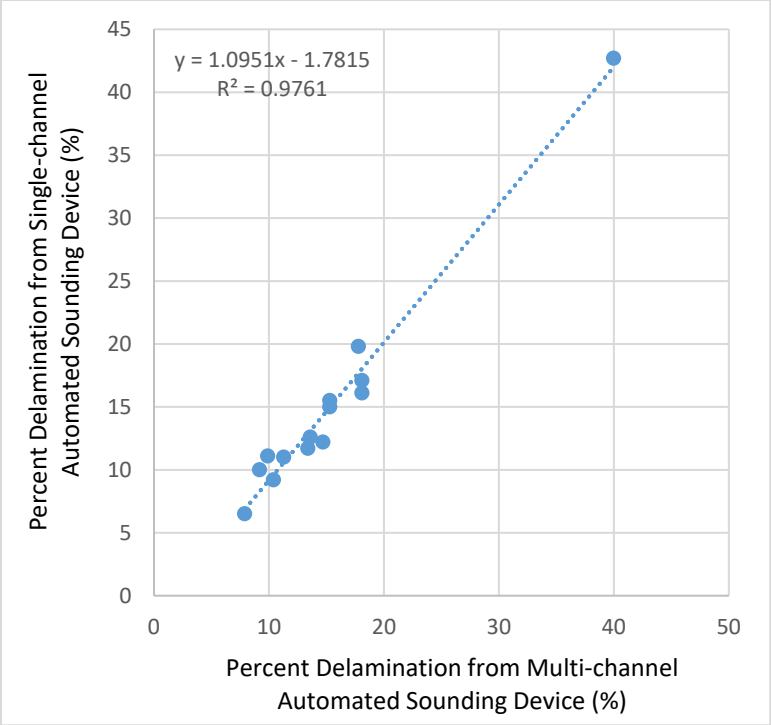

Figure 3-13. Regression analysis for data from both automated sounding devices for the first field demonstration.

Figure 3-14 presents the regression analysis performed for the second set of field demonstrations in Park City, Utah from the data in Tables 3-2 and 3-3. The dashed regression line in Figure 3-14 very closely approximates the line of equality between the two data sets. Furthermore, a regression analysis yielded a comparatively high coefficient of determination, or R^2 value, of 0.8315 for the observed range in delamination from 0.0 to nearly 3.5 percent. Thus, with an average difference of less than 0.3 percent between the two data sets and a maximum difference of less than 1.0 percent for any given deck section, the spatial distributions of delaminations detected using the automated sounding trailer are very similar to those detected using chain dragging. Consequently, any maintenance or rehabilitation strategies developed for these bridge decks from the automated sounding data would be expected to be the same as those developed from the chain dragging data.

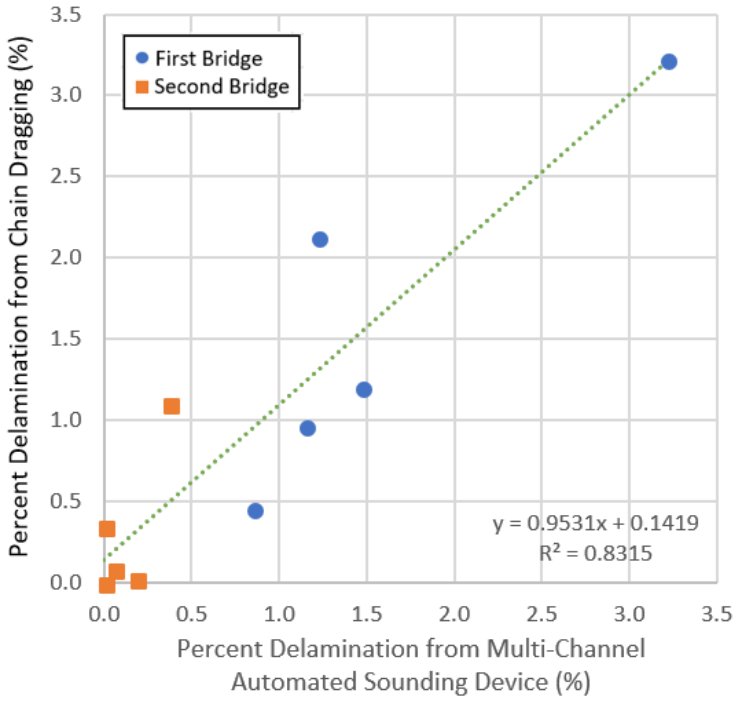

Figure 3-14. Regression analysis of automated sounding data and chain dragging data for the first and second bridges in the second field demonstration.

In general, the minor discrepancies between the results obtained using the automated sounding trailer and chain dragging can be attributed to differences in these methods of inspection. For example, the automated sounding trailer obtains data from individual points on a bridge deck, while chain dragging obtains data from lines or areas, depending on how the chain is dragged. For this reason, the results of the automated sounding trailer can be more negatively influenced than chain dragging by debris on the surface of the deck and/or by transient environmental noise. Therefore, as demonstrated in this research, multiple passes of the automated sounding trailer may be appropriate to ensure comparable deck coverage. Because each pass of the automated sounding trailer can be completed in minutes, with negligible additional data processing time, the process of developing delamination maps using data from multiple passes of the automated sounding trailer, as opposed to a single pass, is still at least an

order of magnitude faster than that associated with chain dragging. In fact, as illustrated by the third bridge evaluated in this research, the automated sounding trailer allows full mapping of delaminations on bridge decks that are too deteriorated for chain dragging to even be completed within a reasonable amount of time.

In this research, BAE thresholds were selected based on a comparison of the data obtained using the automated sounding trailer with those obtained using chain dragging. However, the selected threshold may not apply to all other bridge decks, as changes in deck properties such as thickness and the presence of overlays would be expected to cause changes in the acoustic responses associated with intact and delaminated areas. Because the magnitude of variation in acoustic responses among different bridge decks is unknown, significant field testing will be required to understand the universality of BAE thresholds. Furthermore, the use of statistical methods may also be attractive for deriving BAE thresholds [35]. Finally, the application of machine learning may prove to be an alternative classification scheme that allows automated algorithms to rapidly classify an area of concrete as either delaminated or intact. The apparatus described in this work is a platform with which these additional studies can be completed.

3.4 Conclusion

In this work, a new multi-channel, air-coupled, automated, impact-echo sounding device was designed, constructed, and demonstrated. The apparatus developed in this research includes seven replicated impactor and recording units, a moving trailer platform, a DMI, and signal processing modules. Each mallet is placed on the trailer 61.0 cm from the adjacent mallets, which results in a total trailer width of 3.76 m, or approximately the width of a standard traffic lane, when the trailer is unfolded. In practice, the trailer is towed at a speed of about 0.3 m/s so

that each impactor unit executes an impact every 30 to 60 cm in the travel direction along the bridge deck. A series of computer algorithms is used to determine the presence of delamination on the deck based on the BAE value computed from the acoustic response associated with each impact.

Automation of the sounding process with this device significantly decreases the required inspection time, eliminates the subjectivity associated with traditional sounding methods, and increases safety by substantially reducing the exposure of inspectors to live traffic. Because each pass of the automated sounding trailer can be completed in minutes, the process of developing delamination maps using data from multiple passes of the automated sounding trailer is at least an order of magnitude faster than that associated with chain dragging. In fact, as illustrated by the third bridge of the second field demonstration, the automated sounding trailer allows full mapping of delaminations on bridge decks that are too deteriorated for chain dragging to even be completed within a reasonable amount of time.

For the first and second bridges evaluated in the second field demonstration of this research, which exhibited a range in delamination from 0.0 to nearly 3.5 percent, the spatial distributions of delaminations detected using the automated sounding trailer are very similar to those detected using chain dragging, with an average difference of less than 0.3 percent between the two data sets and a maximum difference of less than 1.0 percent for any given deck section. Therefore, while additional field testing will be required to understand the universality of BAE thresholds, use of the new automated sounding device is recommended for determining the extent of delamination in the process of selecting appropriate maintenance and rehabilitation strategies to maximize performance and minimize overall life-cycle costs of bridge decks.

4 CONCLUSION AND FUTURE WORK

4.1 Results and Discussion

In this work, two complete sounding devices were built and tested with the goal of automating traditional manual sounding inspections that require significant amounts of time. First, a single-channel device was built to test the ability to detect delaminations with an automated mallet and microphone. After successfully locating delaminations on a bridge in Clearfield, Utah, this device was expanded to a multi-channel system with 7 mallet units, each spaced 61-cm apart on a trailer. This multi-channel device could be pulled across a bridge deck and cover an entire traffic lane in one pass. This device was also tested on the same bridge in Clearfield, Utah, as well as 3 other bridges in Park City, Utah. After selecting BAE thresholds for both devices on each bridge, intact and delaminated concrete could be distinguished and delamination percentages estimated for each bridge.

Both devices returned delamination percentage estimates that were highly correlated with the chaining inspection for the first bridge in Clearfield, Utah. In Park City, Utah, only the multi-channel device was used for the field demonstrations and the spatial distributions of delaminations detected using the automated sounding trailer were very similar to those detected using chain dragging. Consequently, any maintenance or rehabilitation strategies developed for these bridge decks from the automated sounding data would be expected to be the same as those developed from the chain dragging data.

In general, the minor discrepancies between the results obtained using the automated sounding devices and chain dragging can be attributed to differences in these methods of inspection. For example, the automated sounding devices obtain data from individual points on a bridge deck, while chain dragging obtains data from lines or areas, depending on how the chain is dragged. Because each pass of the automated sounding trailer can be completed in minutes, with negligible additional data processing time, the process of developing delamination maps using data from multiple passes of the automated sounding devices is at least an order of magnitude faster than that associated with chain dragging. In fact, as illustrated by the third bridge of the second field demonstration, the automated sounding trailer allows full mapping of delaminations on bridge decks that are too deteriorated for chain dragging to even be completed within a reasonable amount of time.

4.2 Future Work

Improvements that can be made to the automated sounding devices mostly deal with accuracy in detecting delaminations. One such improvement would be to increase the number of mallets that are mounted to the 12-foot-wide trailer of the multi-channel device. This would decrease the spacing between each mallet from the current 2-foot spacing. This would mean that small delaminations (less than 2 feet wide) could not as easily pass between the mallets on the trailer and go undetected during the bridge inspection. While a chaining inspection would still provide more comprehensive deck coverage, increasing the resolution of impacts that are generated across the bridge deck would likely increase the accuracy of the delamination percentage estimates.

In this research, BAE thresholds were selected based on a comparison of the data obtained using the automated sounding trailer with those obtained using chain dragging. However, the selected threshold may not apply to all other bridge decks, as changes in deck properties such as thickness and the presence of overlays would be expected to cause changes in the acoustic responses associated with intact and delaminated areas. Because the magnitude of variation in acoustic responses among different bridge decks is unknown, significant field testing will be required to understand the universality of BAE thresholds.

Another attractive approach for computer classification of delaminations is the application of machine learning techniques. Neural networks could have potential for finding other features in a recorded impact that would distinguish intact from delaminated concrete. Implementing a machine learning approach would require a large training data set of recorded impacts from a wide variety of bridges whose delaminations may have differing acoustic properties. The multi-channel device developed in this work has the ability to collect these impacts with which a training data set like this could be constructed.

4.3 Conclusion

The devices developed in this work demonstrate the utility of automation in current bridge inspection processes. Both single-channel and multi-channel devices were able to excite delaminations on bridge decks by means of automated mallets and record the acoustic responses with microphones. The computer algorithms used for processing the acoustic data were able to classify the concrete that was impacted as either intact or delaminated. The automated sounding devices were able to complete the deck inspections at least 1 order of magnitude faster than the chain drag inspections, not including the manual entering of chain drag information at the office.

Automation of traditional sounding techniques significantly decreases the standard bridge deck inspection time, eliminates the subjectivity involved in current inspection methods, and increases safety by substantially reducing the exposure of inspectors to live trafficking. Departments of Transportation could save significant amounts of time and money by implementing automated inspection technologies. The documented technology developed in this thesis demonstrates how robotics, automation, and signal processing can be used to solve challenging problems in the field of civil infrastructure.

REFERENCES

[1] 2017 ASCE Infrastructure Report Card, https://www.infrastructurereportcard.org/cat-item/bridges/.

[2] J. Hema, W. S. Guthrie, and F. S. Fonseca, “Concrete Bridge Deck Condition Assessment and Improvement Strategies.” Report UT-04.16. *Utah Department of Transportation*, Salt Lake City, UT, November 2004.

[3] W.S. Guthrie, and R. S. Tuttle, “Condition Analysis of Concrete Bridge Decks in Utah.” Report UT-06.01. *Utah Department of Transportation,* Salt Lake City, UT, February 2006.

[4] J. F. Young, S. Mindess, R. J. Gray, and A. Bentur, “The Science and Technology of Civil Engineering Materials.” Upper Sadde River, NJ: Prentice-Hall, Inc. 1998.

[5] M. Sansalone, "Impact-echo: The complete story," *ACI Structural Journal,* vol. 94, pp. 777-786, Nov-Dec 1997.

[6] M. Sansalone, and N. J. Carino, “Detecting Delaminations in Concrete Slabs with and without Overlays Using the Impact-Echo Method,” *ACI Materials Journal,* vol. 86, No. 2, pp. 175-184, Mar-Apr 1989.

[7] C. M. Hsiao, C. C. Cheng, T. H. Liou, and Y. T. Juang, “Detecting flaws in concrete blocks using the impact-echo method,” *NDT&E International*, vol. 41, pp. 98-107, Mar 2008.

[8] M. T. A. Chaudhary, “Effectiveness of Impact Echo testing in detecting flaws in prestressed concrete slabs,” *Construction and Building Materials*, vol. 47, pp. 753-759, 2013.

[9] J. S. Popovics and J. L. Rose, "A new approach for the analysis of impact-echo data," *Review of Progress in Quantitative Nondestructive Evaluation,* vol. 12, 1993.

[10] N. J. Carino, “The Impact-Echo Method: An Overview,” *ASCE World Structural Engineering Conference*, May 2001.

[11] S. Kee and N. Gucunski, "Interpretation of Flexural Vibration Modes from Impact-Echo Testing," *J. Infrastruct. Syst.*, 04016009, 1-10, 2016.

[12] J. Y. Zhu and J. S. Popovics, “Non-contact detection of surface waves in concrete using an air-coupled sensor,” *AIP Conference Proceedings* (2002); doi: 10.1063/1.1472940

[13] J. Y. Zhu and J. S. Popovics, “Air-Coupled Impact-Echo Method for NDT of Concrete,” *AIP Conference Proceedings* (2006); doi: 10.1063/1.2184681

[14] J. Y. Zhu and J. S. Popovics, "Imaging concrete structures using air-coupled impact-echo," *Journal of Engineering Mechanics-ASCE,* vol. 133, pp. 628-640, Jun 2007.

[15] J. S. Popovics, T. Oh, and S. Ham, “Effective visualization of impact-echo data for bridge deck NDE,” AIP Conference Proceedings, vol. 1430, pp. 1681-1688, 2012.

[16] S. W. Shin, J. S. Popovics, and T. Oh, “Cost Effective Air-Coupled Impact-Echo Sensing for Rapid Detection of Delamination Damage in Concrete Structures,” *Advances in Structural Engineering*, vol. 15, pp. 887-895, Jun 2012.

[17] S. H. Kee, T. Oh, J. S. Popovics, R. W. Arndt, and J. Y. Zhu, “Nondestructive Bridge Deck Testing with Air-Coupled Impact-Echo and Infrared Thermography,” *Journal of Bridge Engineering*, vol. 17, pp. 928-939, Nov-Dec 2012.

[18] D. Algernon, H. Ernst, and K. Dressler, “Signal Processing for Air-Coupled Impact-Echo using Microphone Arrays,” presented at the 18th World Conference on Nondestructive Testing, Durban, South Africa, 2012.

[19] T. Oh, “Defect Characterization in Concrete Elements Using Vibration Analysis and Imaging,” *Department of Civil Engineering – University of Illinois at Urbana-Champaign,* Dissertation, 2012.

[20] N. Gucunski, A. Imani, F. Romero, S. Nazarian, D. Yuan, and H. Wiggenhauser*,* et al., “Nondestructive testing to identify concrete bridge deck deterioration.” Washington, D.C. : Transportation Research Board, 2013.

[21] B. A. Mazzeo, A. N. Patil, R. C. Hurd, J. M. Klis, T. T. Truscott, and W. S. Guthrie, "Air-Coupled Impact-Echo Delamination Detection in Concrete Using Spheres of Ice for Excitation," *Journal of Nondestructive Evaluation,* pp. 1-10, 2013/12/07 2013.

[22] B. A. Mazzeo, A. N. Patil, and W. S. Guthrie, "Acoustic impact-echo investigation of concrete delaminations using liquid droplet excitation," *NDT&E International,* vol. 51, pp. 41-44, 2012.

[23] N. Gucunski, F. Romero, S. Kruschwitz, R. Feldmann, A. Abu-Hawash, and M. Dunn, “Multiple Complementary Nondestructive Evaluation Technologies for Condition Assessment of Concrete Bridge Decks,” Transportation Research Record, vol. 2201, pp. 34-44, 2010.

[24] Y. Tinkey, L. D. Olson, Olson Engineering, “Vehicle-Mounted Bridge Deck Scanner,” *Transportation Research Board: Highway IDEA Program,* Project 132, Aug 2010.

[25] J. S. Popovics, “Investigation of a Full-Lane Acoustic Scanning Method for Bridge Deck Nondestructive Evaluation,” *Transportation Research Board: Highway IDEA Program,* Project 134, Nov 2010.

[26] J. Y. Zhu and J. S. Popovics, "Imaging concrete structures using air-coupled impact-echo," *Journal of Engineering Mechanics-ASCE,* vol. 133, pp. 628-640, Jun 2007.

[27] S. W. Shin, J. S. Popovics, and T. Oh, “Cost Effective Air-Coupled Impact-Echo Sensing for Rapid Detection of Delamination Damage in Concrete Structures,” *Advances in Structural Engineering*, vol. 15, pp. 887-895, Jun 2012.

[28] G. Zhang, R. S. Harichandran, P. Ramuhalli, “An automatic impact-based delamination detection system for concrete bridge decks,” *NDT&E International,* vol. 45, pp. 120-127, 2012.

[29] H. Sun, J. Zhu, S. Ham, “Acoustic evaluation of concrete delaminations using ball-chain impact excitation,” *The Journal of the Acoustical Society of America,* vol. 141, May 2017.

[30] W. S. Guthrie, J. Larsen, J. Baxter, B. A. Mazzeo, “Automated Air-Coupled Impact-Echo Testing of a Concrete Bridge Deck from a Continuously Moving Platform,” UNDER REVIEW.

[31] B. A. Mazzeo, J. Larsen, J. McElderry, and W. S. Guthrie, “Rapid multichannel impact-echo scanning of concrete bridge decks from a continuously moving platform,” AIP Conference Proceedings 1806, 080003, 2017.

[32] B. A. Mazzeo, T. T. Truscott, and W. S. Guthrie, "Signal processing of acoustic impact response for reinforced concrete testing using paintballs and airsoft pellets for excitation," *Audio and Acoustic Signal Processing Technical Committee Newsletter,* vol. 1, 2014.

[33] T. Oh, J. S. Popovics, and S. Sim, "Analysis of vibration for regions above rectangular delamination defects in solids," *Journal of Sound and Vibration,* vol. 332, pp. 1766-1776, 4/1/ 2013.

[34] S. Ham, J. S. Popovics, “Application of Micro-Electro-Mechanical Sensors Contactless NDT of Concrete Structures,” *Sensors,* vol. 15, Issue 4, 10.3390/s150409078, Apr 2015.

[35] L. Hendricks, W. S. Guthrie, B. A. Mazzeo, “Implementing statistical analysis in multi-channel acoustic impact-echo testing of concrete bridge decks: Determining thresholds for delamination detection,” AIP Conference Proceedings 1949, 040005, 2018.

APPENDIX A. SCHEMATICS AND CODE

Example image of mallet striking the concrete with microphones recording the impact audio

Daughter board mounted on a FRDM-K64F development board for mallet control and audio recording

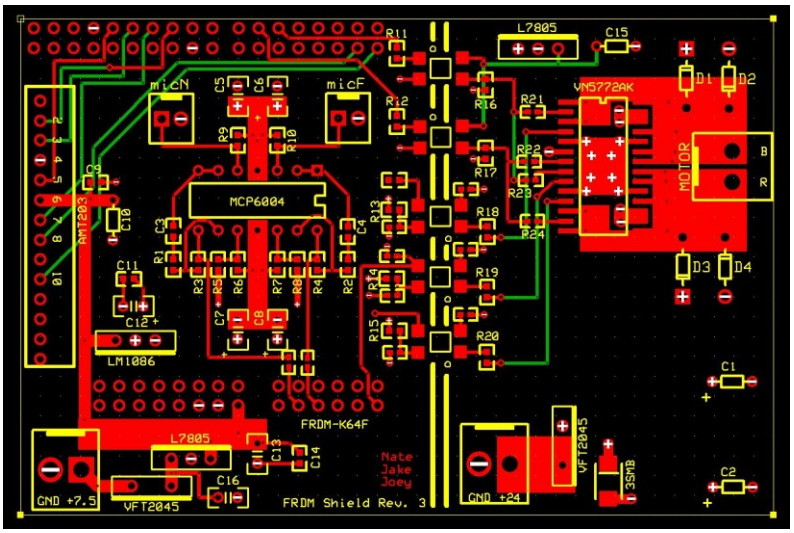

Parts list for daughter board mounted to FRDM-K64F

Part	Digikey P/N	Shield Reference	Quantity
3.3V LDO	LM1086IT-3.3/NOPB-ND	LM1086	1
5V LDO	497-1443-5-ND	L7805	2
H Bridge Motor Driver	497-11677-1-ND	VN5772AK	1
Battery diode - 45V - 20A	VFT2045BP-M3/4W-ND	VFT2045	2
33V - 3W Zener Diode	3SMBJ5937BTPMSCT-ND	3SMB	1
Optoisolator	425-2108-1-ND	PC3H71	5
FRDM-K64F	FRDM-K64F-ND	FRDM-K64F	1
600V - 1A Flyback diode	1N4005-TPMSCT-ND	D1,D2,D3,D4	4
AMT203-V	102-2050-ND	AMT203	1
Electret Condensor Mic	102-1722-ND	micN,micF	2
Op Amp	MCP6004-I/P-ND	MCP6004	1
1A Fuse - 32 VDC	F4191-ND		
5A Fuse - 32 VDC	F4197-ND		
Resistors			
10kOhm RES 0603	BYU Campus Shop	R5,R6,R7,R8,R9,R10	6
31.6 kOhm RES 0603	BYU Campus Shop	R3,R4	2
53kOhm RES 0603	BYU Campus Shop	R1,R2	2
909 Ohm	BYU Campus Shop	R11,R12	2
0 ohm RES 0402	BYU Campus Shop	R13,R14,R15	3
Decide later	BYU Campus Shop	R16,R17,R18,R19,R20	5
10k RES 0402	BYU Campus Shop	R21,R22,R23,R24	4
Capacitors			
0.1uF CAP	BYU Campus Shop	C5,C7	
1uF 10V CAP	1276-1946-1-ND	C3,C4	2
10uF CAP	BYU Campus Shop	C6,C8,C10,C9,C11	
180uF CAP	BYU Campus Shop	C1,C2	2
Connectors			
Large connector	BYU Campus Shop	5v,24v,motor	3
Small connector	BYU Campus Shop	micN,micF	2
10 Position Vertical Header Connector	A1925-ND		
2 Position Connection Housing	WM2100-ND		
2 Position Vertical Header Connector	WM4620-ND		
2 Position Reception Connector	A30994-ND		
2 Position Vertical Header Connector	A1921-ND		

Daughter board mounted on a FRDM-K64F development board for DMI

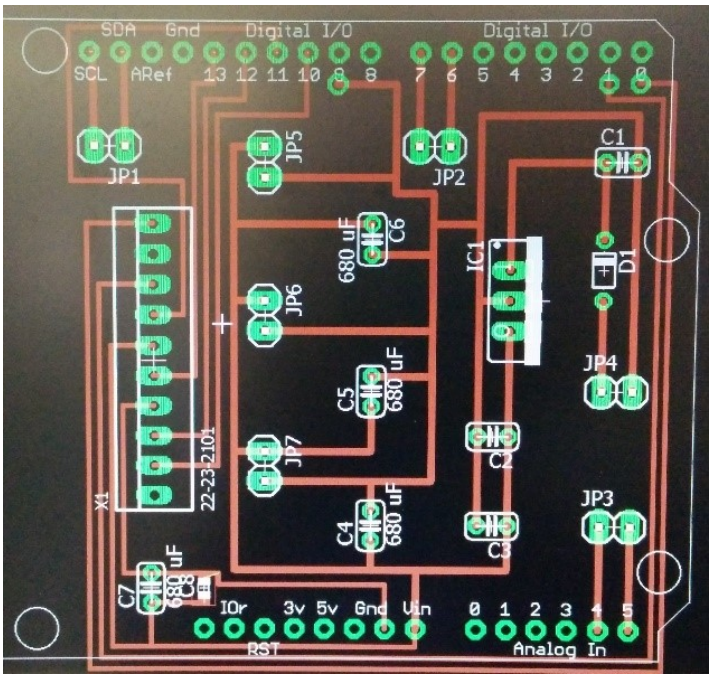

Preliminary mallet design drawing

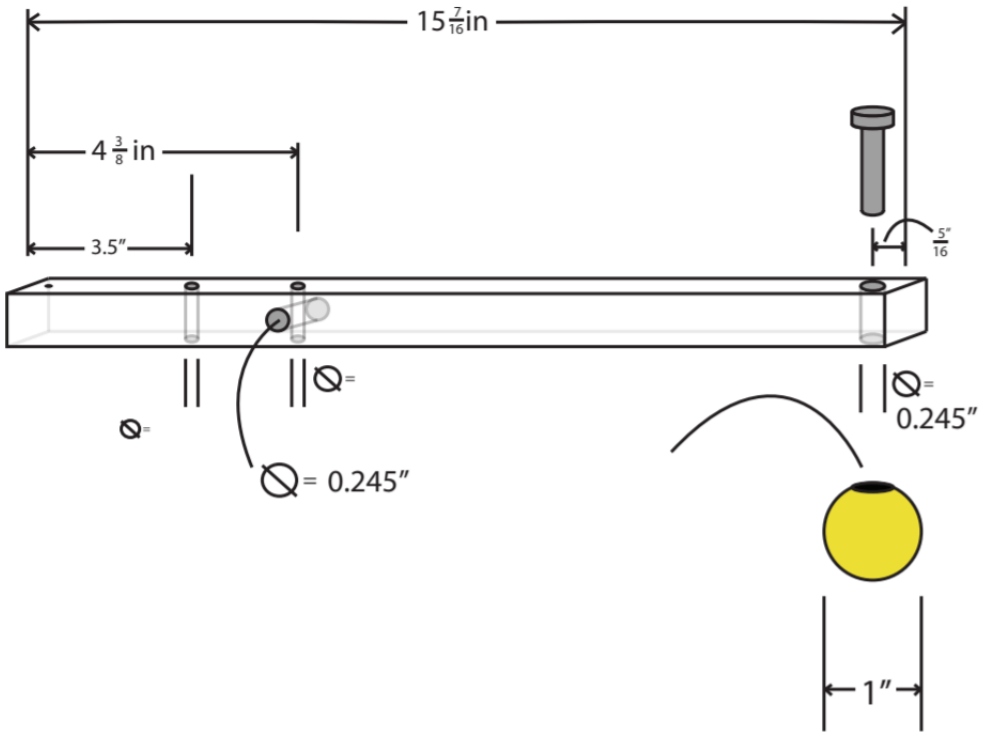

Drawing for aluminum plate with mounting holes for mallet and other components

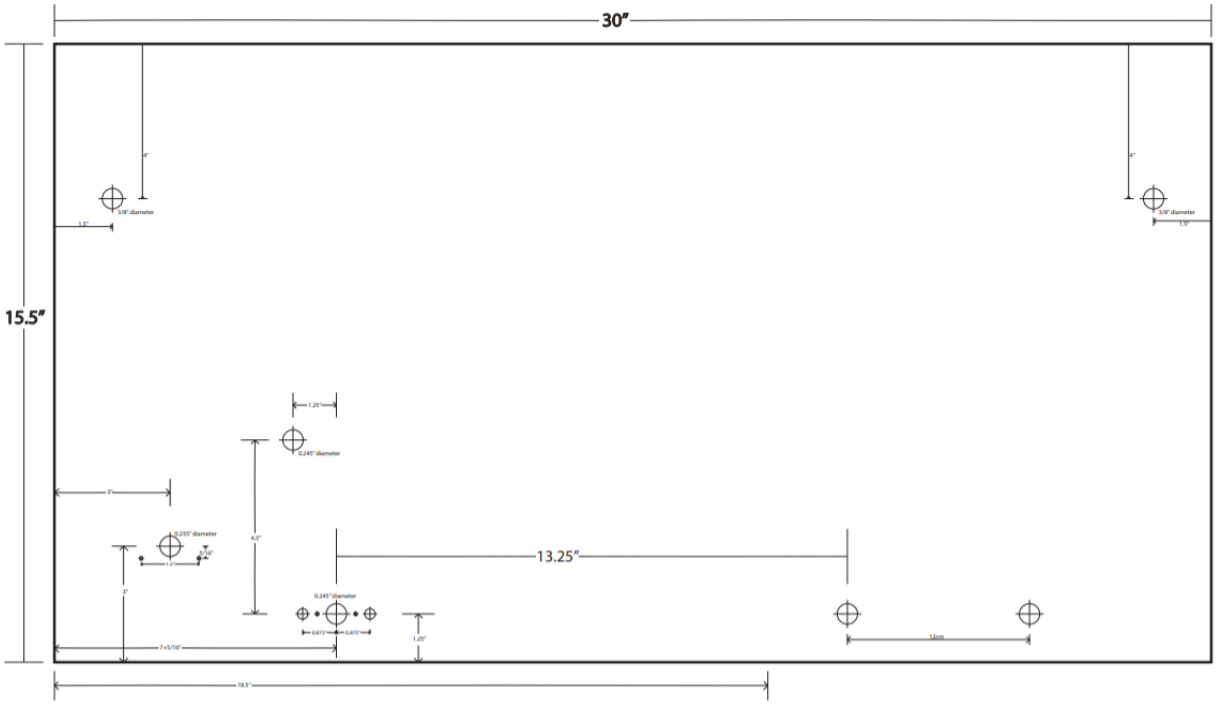

Drawings of 3D printed microphone box

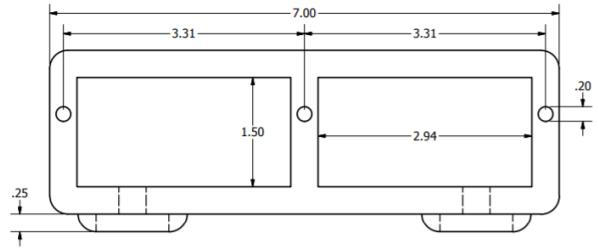

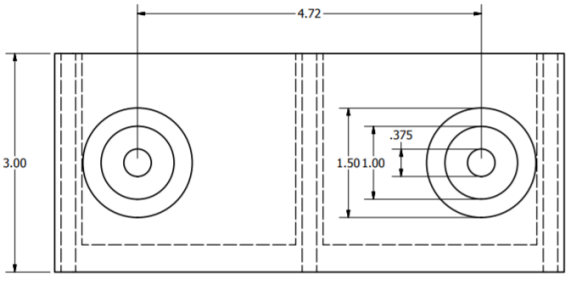

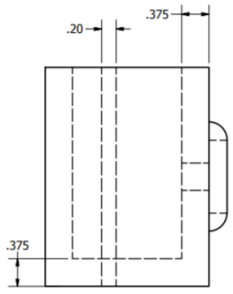

Drawings for 3D printed snail cam that controls the impacts

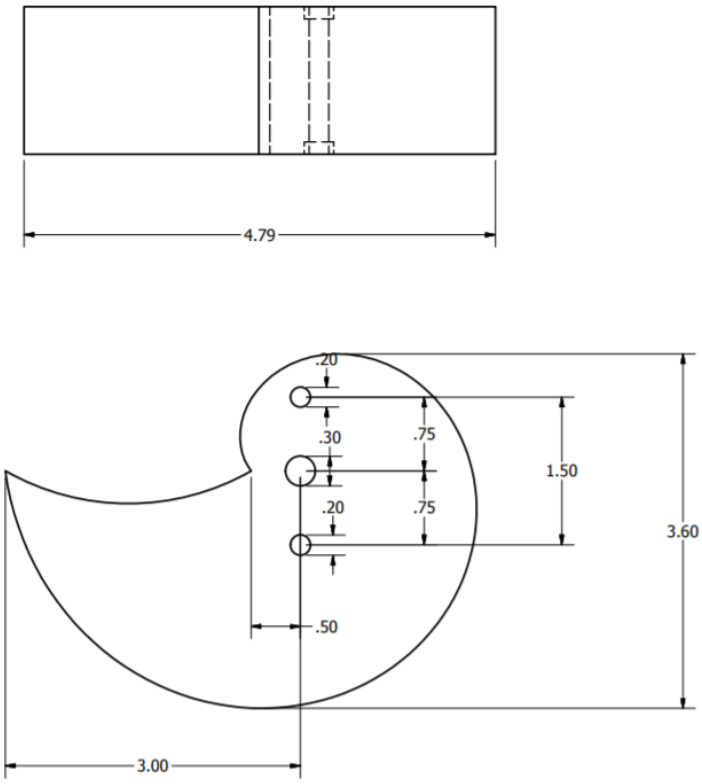

Drawing for unfolded trailer layout and construction

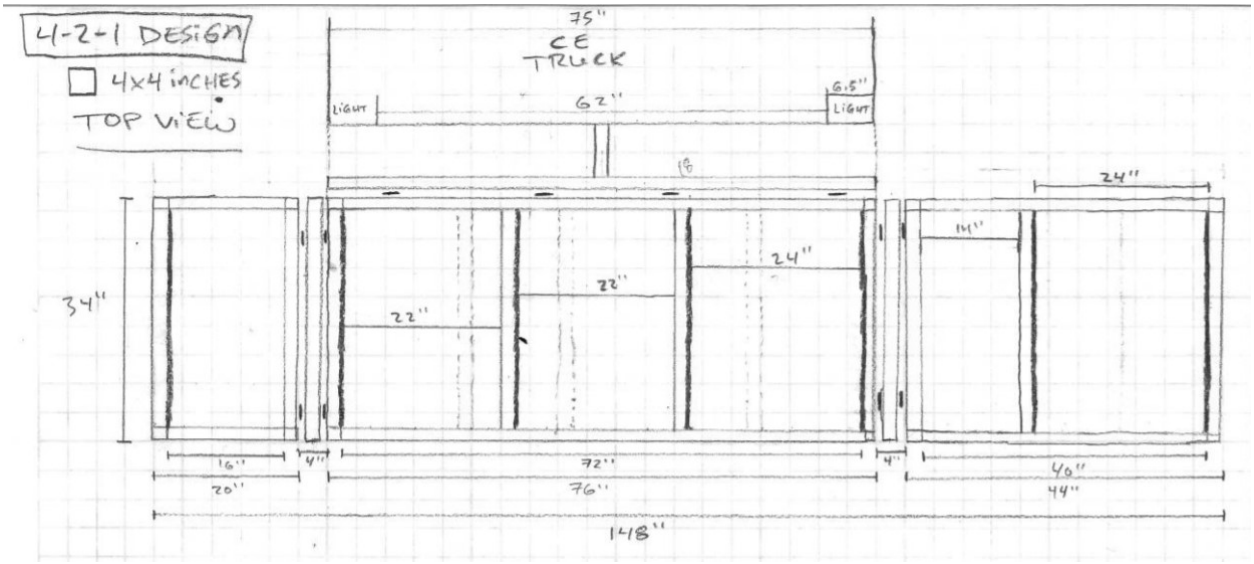

Drawings for folded trailer layout and construction with hitching attachment for winching

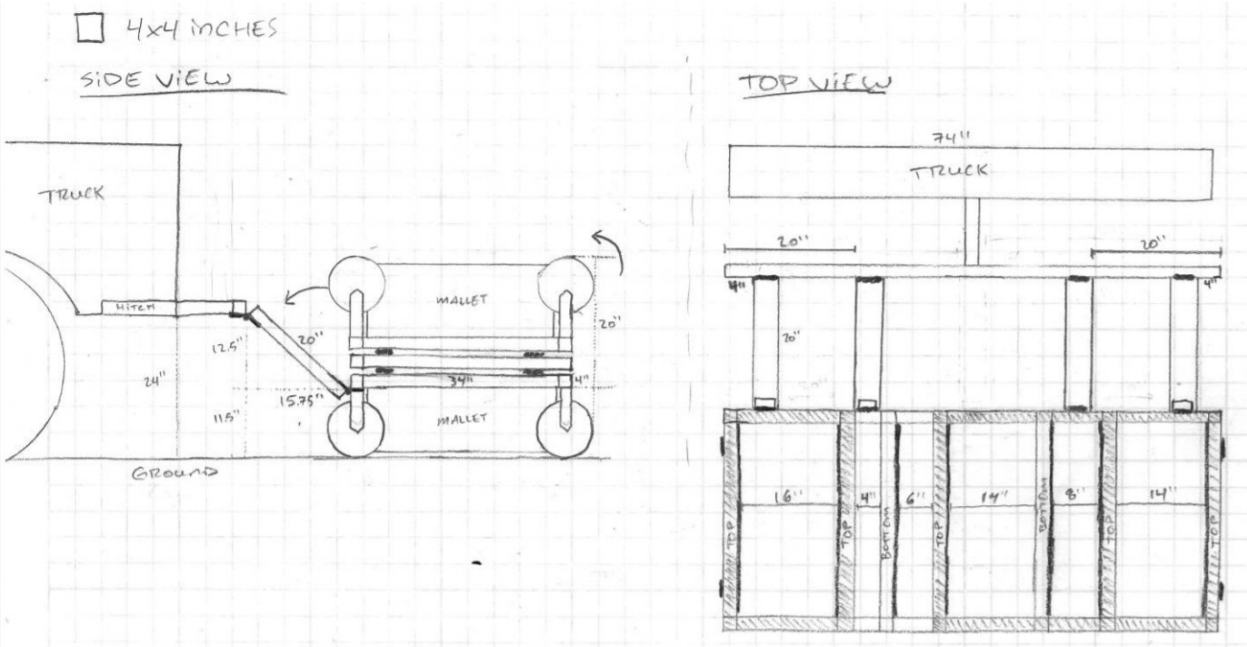

MEMS PDM microphone with circuit for wiring contacts to FRDM board connector

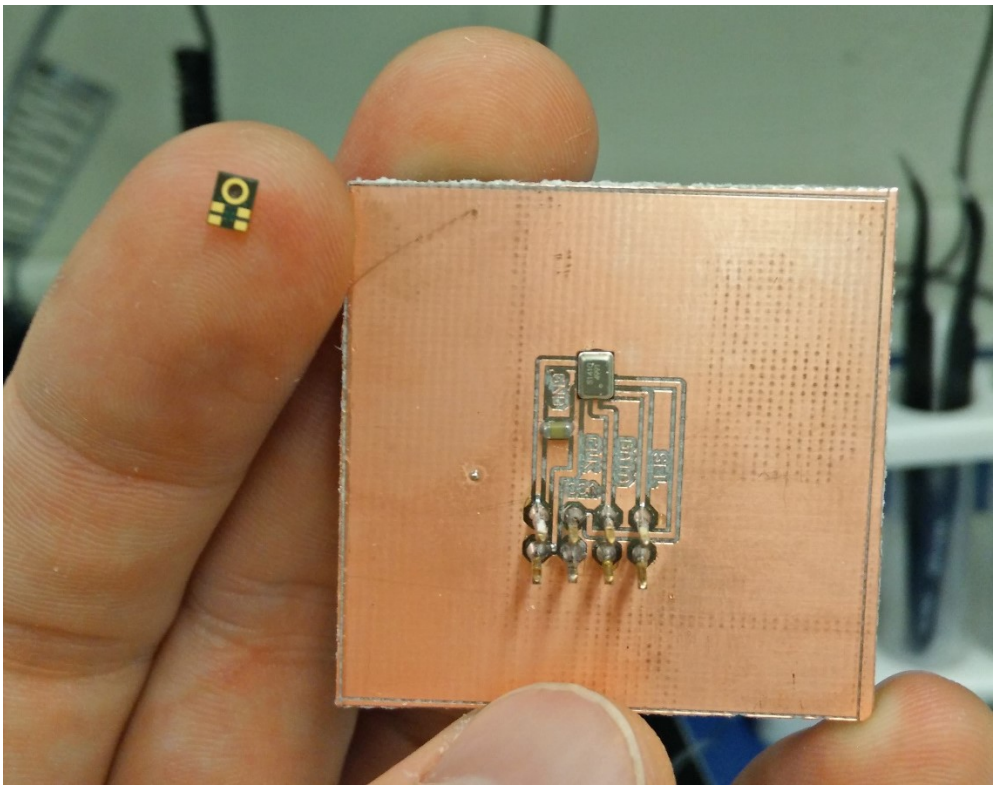

C++ Code running on FRDM boards for controlling the mallet firing and reset as well as the audio recording of the impacts

main.cpp

```
// MalletFirmware, this is the real deal version
/* * * * * * * * * * * * * * * * * * * * * * * * * * * * * * * *
 *
 *        Pinout for FRDM-k64f
 *                          J2
 *                          X X
 *                          X X
 *                          X X
 *        J3                  X X GND
 *        X X                   X X SCLK
 *        X X                   X X MISO
 *        X X                   X X MOSI
 *        X X                   X X CS
 *        X X                 GND X X
 *     GND X X                    X X
 *     GND X X
 *    5Vin X X                    J1
 *                          X X
 *        J4                  X X motorA
 *        X X                   X X motorB
 *    mic1 X X                    X X
 *    mic2 X X                    X X
 *        X X                   X X
 *        X X               quadA X X
 *        X X               quadB X X
 *
 * * * * * * * * * * * * * * * * * * * * * * * * * * * * * * * */

#include "mbed.h"
#include <string>

// Hardware delays
#include "pause.cpp"

// Ethernet
#include "EthernetInterface.h"

// Angle encoder and motor control
#include "AngleEncoder.h"
#include "MotorControl.h"

// Sampling
#include "Sample/dma.h"
#include "Sample/pdb.h"
#include "Sample/quad.h"

#include "debug.cpp"

#ifdef DEBUG_ON
#undef DEBUG_ON
```

```
#endif
#define DEBUG_ON 1 // 1 or 0

// Settings for each mallet
#define MAX_CLIENTS  2          // set the max number of clients to at least 2 (first client is MATLAB, second is
the distance unit)

// Ethernet
#define LEN_PACKET 1460
#define NUM_PACKETS ((TOTAL_SAMPLES_MIC+TOTAL_SAMPLES_ANGLE)/LEN_PACKET)
#define GATEWAY "169.254.225.1" // set to match your computer
#define MASK "255.255.0.0"      // set to match your computer (probably does already)
#define IP_LAPTOP "169.254.225.205"
#define IP_DMI    "169.254.225.220"


#define SAMPLE_FREQ 3750000 // 3.75 MHz
// for debug purposes
Serial pc(USBTX, USBRX);

// motor control
MotorControl motor(PTC2, PTA2, 2000, 25); // cw, ccw, period_us, safetyPeriod_us

//DigitalOut sel(PTC12); // pull up resistor used instead
//DigitalIn temp_trigger(PTB2); // for simultaneous trigger

char buffer[LEN_PACKET]; // general purpose tx/rx buffer
char status[LEN_PACKET]; // tx buffer that contains the status for the entire mallet system

int NUM;
int PORT = 55000;

// Declaration of functions
void clearBuffer();
bool syncAngles();
void pdm_init();
int spi_start();


using namespace std;

int main() {
   led_blue = 1;
   led_green = 1;
   led_red = 0;

   if(SIM_UIDH == 0x001bffff && SIM_UIDML == 0x4d441504 && SIM_UIDL == 0x9013001C) NUM = 1;
   else if(SIM_UIDH == 0x0016ffff && SIM_UIDML == 0x4d441504 && SIM_UIDL == 0x90110007) NUM =
2;
   else if(SIM_UIDH == 0x0023ffff && SIM_UIDML == 0x4e453103 && SIM_UIDL == 0x70060023) NUM = 3;
   else if(SIM_UIDH == 0x0010ffff && SIM_UIDML == 0x4e453103 && SIM_UIDL == 0x7006001f) NUM = 4;
   else if(SIM_UIDH == 0x0025ffff && SIM_UIDML == 0x4d441504 && SIM_UIDL == 0x90120003) NUM =
5;
   else if(SIM_UIDH == 0x0018ffff && SIM_UIDML == 0x4d441504 && SIM_UIDL == 0x90120008) NUM =
6;
   else if(SIM_UIDH == 0x0015ffff && SIM_UIDML == 0x4e453103 && SIM_UIDL == 0x60010012) NUM = 7;
```

```
else NUM = -1;
PORT += NUM;

pc.baud(230400);
pc.printf("\r\n\n\n\n\nStarting M%i\r\n",NUM);

pc.printf("SIM_UIDH  0x%08x\r\n", SIM_UIDH);
pc.printf("SIM_UIDMH 0x%08x\r\n", SIM_UIDMH);
pc.printf("SIM_UIDML 0x%08x\r\n", SIM_UIDML);
pc.printf("SIM_UIDL  0x%08x\r\n", SIM_UIDL);

// Give everything lower priority
for(int i = 0; i < 86; i++)
{
   if(NVIC_GetPriority((IRQn_Type) i) == 0) NVIC_SetPriority((IRQn_Type) i, 2);
}

// Give hardware associated with
// sampling the highest priority
//NVIC_SetPriority(ADC1_IRQn,0);
//NVIC_SetPriority(ADC0_IRQn,0);
//NVIC_SetPriority(PDB0_IRQn,0);
NVIC_SetPriority(DMA0_IRQn,0);
NVIC_SetPriority(DMA1_IRQn,0);
NVIC_SetPriority(DMA2_IRQn,0);

NVIC_SetPriority(ENET_1588_Timer_IRQn,1);
NVIC_SetPriority(ENET_Transmit_IRQn,1);
NVIC_SetPriority(ENET_Receive_IRQn,1);
NVIC_SetPriority(ENET_Error_IRQn,1);


// The ethernet setup must be within the first few lines of code, otherwise the program hangs
EthernetInterface interface;

if(NUM == 1)      interface.init("169.254.225.221", MASK, GATEWAY);
else if(NUM == 2) interface.init("169.254.225.222", MASK, GATEWAY);
else if(NUM == 3) interface.init("169.254.225.223", MASK, GATEWAY);
else if(NUM == 4) interface.init("169.254.225.224", MASK, GATEWAY);
else if(NUM == 5) interface.init("169.254.225.225", MASK, GATEWAY);
else if(NUM == 6) interface.init("169.254.225.226", MASK, GATEWAY);
else if(NUM == 7) interface.init("169.254.225.227", MASK, GATEWAY);

interface.connect();

led_green = 0;

pc.printf("IP Address is: %s\n\r", interface.getIPAddress());
pc.printf("Port is: %i\n\r", PORT);
ENET_TIPG = 0x08; // minimum time between TCP packets

// ethernet setup failed for some reason.  Flash yellow light then uC resets itself
if(interface.getIPAddress() == 0)
{
   for(int i = 0; i < 5; i++)
   {
```

```
        // flash yellow LED
        led_red = 0;
        led_green = 0;
        pause_ms(500);
        led_red = 1;
        led_green = 1;
        pause_ms(1000);
    }
    NVIC_SystemReset();
}

quad_init(); // initialize FTM2 quadrature decoder
quad_invert();

pc.printf("TOTAL_SAMPLES_MIC = %i\r\n", TOTAL_SAMPLES_MIC);
pc.printf("TOTAL_SAMPLES_ANGLE = %i\r\n", TOTAL_SAMPLES_ANGLE);
#ifdef MEMS
pc.printf("Setup PDM for MEMS microphone\r\n");
// setup the SPI1 port
// -The frequency, polarity/phase, and polarity of the MEMS
//  microphone are all interrelated.  Don't modify any of them.
SPI spi1(PTD6, PTD7, PTD5, PTD4); // for some reason, the code freezes if this is declared as global
spi1.frequency(SAMPLE_FREQ);
spi1.format(16,1); // 16 bit, POL = 0, PHA = 1

// change SPI1 to work with PDM and setup DMA
pdm_init();
dma_spi_init();

#else
pc.printf("Setup ADCs for analog microphones\r\n");
adc_init(); // initialize ADCs (always initialize adc before dma)
dma_adc_init(); // initializes DMAs
#endif

pdb_init(); // initialize PDB0 as the timer for DMA2 to read the FTM (quadrature decoder)

syncAngles();

TCPSocketServer server;
server.bind(PORT);
server.listen(MAX_CLIENTS);

led_green = 1;
led_red = 1;
led_blue = 1;
pc.printf("Server started\r\n");
pc.printf("%c",0x07); // sound bell (if TeraTerm is open, you'll hear a sound)

pc.printf("Calibrating motors\r\n");
//motor.calibrate();

bool dataReady = false;
while(true) { // tcp connect/disconnect loop
    clearBuffer();
    TCPSocketConnection laptop;
```

```
server.accept(laptop);
laptop.set_blocking(false, 9000); // timeout after 9s

bool ipVerified = true;
string ipAddress = laptop.get_address();
if(ipAddress != IP_LAPTOP) ipVerified = false;
int n;
while(true) { // rx/tx loop
   n = laptop.receive(buffer,LEN_PACKET); // this operation times out after 1.5s
   if(n <= 0) break; // exit rx/tx loop

   if(!ipVerified){
      clearBuffer();
      sprintf(buffer,"Incorrect IP address");
      n = laptop.send(buffer,LEN_PACKET);
      pc.printf("%s\r\n");
      break; // exit rx/tx loop
   }

   if(buffer[0] == ':' && ipVerified) {
      switch(buffer[1])
      {
         // take sample
         case 'M': // :M0.0000000000.0000000000  // yellow
         case 2:
         {
            if( (buffer[2]-0x30) == NUM ) // has correct malletID number
            {
               led_green = 0;
               led_red = 0;
               if(!motor.getCalibration()){
                  clearBuffer();
                  sprintf(buffer,"Calibrate motor before attempting reset");
                  n = laptop.send(buffer,LEN_PACKET);
                  DEBUG printf("Calibrate motor before attempting reset\r\n");
                  break;
               }
               n = laptop.send(buffer,LEN_PACKET);

               // update angle
               bool success = syncAngles();
               motor.releaseMallet();

               // wait for mallet to fall a certain distance (max wait time is 40ms)
               int start_height = quad_read();
               for(int i = 0; i < 40; i++){
                  pause_ms(1);
                  if( (quad_read()-start_height) > 180 ) break;
               }
               DEBUG printf("Start %i\t Stop %i\r\n", start_height, quad_read());


            }
         }
         case 'L':
         case 'l':
```

```
            {
               // start sampling
               pdb_start();
               DEBUG printf("Start SPI\r\n");

               //int returnVar = spi1.write(0x00f0);
               int returnVar = spi_start();

               // keep waiting for sampling to complete
               for(int i = 0; i < 30; i++) { // timeout loop. sampling takes approx 137ms, this loop takes
30*5ms=150ms
                  if(dma_done) break;
                  pc.printf("sampling...\r\n");
                  pause_ms(5);
               }

               dataReady = true;

               // reset mallet
               DEBUG printf("ResetMallet\r\n");
               motor.resetMallet();

               // turn off all indicator LEDs
               led_red = 1;
               led_green = 1;
               led_blue = 1;
               break;
            }
            case 'N':
            case 'n':
            case 0:
            {
               clearBuffer();
               sprintf(buffer,"M%i",NUM);
               n = laptop.send(buffer,LEN_PACKET);
               pc.printf("%s\r\n",buffer);
               break;
            }
            /*********************************************************************
            * The code below is for testing and troubleshooting.  Don't delete. *
            *********************************************************************/
            case 'p':
            case 13:
            {
               clearBuffer();
               sprintf(buffer,"Resetting M%i",NUM);
               n = laptop.send(buffer,LEN_PACKET);
               pc.printf("%s\r\n",buffer);
               pause_ms(200);
               NVIC_SystemReset();
               break;
            }
            case 'B':
            case 'b':
            case 6:
            {
```

```
    clearBuffer();
    if(led_blue){
        led_blue = 0;
        sprintf(buffer,"LED blue = ON");
    }
    else {
        led_blue = 1;
        sprintf(buffer,"LED blue = OFF");
    }
    n = laptop.send(buffer,LEN_PACKET);
    pc.printf("%s\r\n",buffer);
    break;
}
case 'R':
case 'r':
case 7:
{
    clearBuffer();
    if(led_red){
        led_red = 0;
        sprintf(buffer,"LED red = ON");
    }
    else {
        led_red = 1;
        sprintf(buffer,"LED red = OFF");
    }
    n = laptop.send(buffer,LEN_PACKET);
    pc.printf("%s\r\n",buffer);
    break;
}
// test angle encoder
case 'W':
{
    int16_t cow = 5;
    double distance = 0.0;
    distance = double(cow)*.393701;
    clearBuffer();
    sprintf(buffer, "Distance: %f in\r\n", distance);
}
case 'w': // reads 0 unless the counter is running
{
    clearBuffer();
    sprintf(buffer,"PDB: %i",PDB0_CNT);
    pc.printf("%s\r\n",buffer);
    n = laptop.send(buffer,LEN_PACKET);
    break;
}
case 'A':
case 'a': // set zero
case 12:
{
    clearBuffer();
    if(angle_encoder.set_zero()) {
        quad_update(0);
        sprintf(buffer,"Zero set");
    }
```

```
    else sprintf(buffer,"Zero NOT set");
    n = laptop.send(buffer,LEN_PACKET);
    pc.printf("%s\r\n",buffer);
    break;
}
case 'S':
case 's': // perform "no operation", which returns 0xa5
{
    clearBuffer();
    sprintf(buffer,"NOP: %x",angle_encoder.nop());
    n = laptop.send(buffer,LEN_PACKET);
    pc.printf("%s\r\n",buffer);
    break;
}
case 'D':
case 'd': // read absolute and relative angles
case 5:
{
    clearBuffer();
    sprintf(buffer,"Angle: %i %i",angle_encoder.absolute_angle(),quad_read());
    n = laptop.send(buffer,LEN_PACKET);
    pc.printf("%s\r\n",buffer);
    break;
}
case 'F':
case 'f':
{
    clearBuffer();
    sprintf(buffer,"Quad Cnt: %i", quad_read());
    n = laptop.send(buffer,LEN_PACKET);
    pc.printf("%s\r\n",buffer);
    break;
}
case 'G':
case 'g': // sync relative angle with absolute angle
case 11:
{
    clearBuffer();
    bool success = syncAngles();
    if(success) sprintf(buffer,"Angles synchronized");
    else sprintf(buffer,"Could not read absolute angle");
    n = laptop.send(buffer,LEN_PACKET);
    pc.printf("%s\r\n",buffer);
    break;
}


// test motor
case 'Z':
case 'z': // release the mallet
case 8:
{
    clearBuffer();
    sprintf(buffer,"Release mallet");
    n = laptop.send(buffer,LEN_PACKET);
    pc.printf("%s\r\n");
```

```
    bool success = syncAngles();
    if(success) {
        motor.releaseMallet();
        pc.printf("Angles synchronized");
    }
    else pc.printf("Could not read absolute angle");
    break;
}
case 'X':
case 'x': // reset the mallet
case 10:
{
    clearBuffer();
    if(!motor.getCalibration()){
        sprintf(buffer,"Calibrate motor before attempting reset");
        n = laptop.send(buffer,LEN_PACKET);
        pc.printf("%s\r\n",buffer);
        break;
    }
    else {
        sprintf(buffer,"Reset mallet");
        n = laptop.send(buffer,LEN_PACKET);
        pc.printf("%s\r\n",buffer);
        motor.resetMallet();
    }
    break;
}

case 'C':
case 'c': // calibrate the mallet
case 1:
{
    clearBuffer();
    bool success = syncAngles();
    if(success){
        sprintf(buffer,"Calibrate motor/cam reset");
        n = laptop.send(buffer,LEN_PACKET);
        pc.printf("%s\r\n",buffer);
        motor.calibrate();
    }
    else{
        sprintf(buffer,"Could not read absolute angle");
        n = laptop.send(buffer,LEN_PACKET);
        pc.printf("%s\r\n",buffer);
    }
    break;
}

case 'V':
case 'v': // release and reset the mallet
{
    clearBuffer();
    if(!motor.getCalibration()){
        sprintf(buffer,"Calibrate motor before attempting reset");
        n = laptop.send(buffer,LEN_PACKET);
```

```
                    pc.printf("%s\r\n",buffer);
                    break;
                }

                sprintf(buffer,"Release/Reset mallet");
                n = laptop.send(buffer,LEN_PACKET);
                pc.printf("%s\r\n");

                bool success = syncAngles();
                if(success) {
                    motor.releaseMallet();
                    pause_us(TOTAL_SAMPLES_MIC*10);
                    motor.resetMallet();
                }
                else {
                    pc.printf("Could not read absolute angle");
                    break;
                }
                break;
            }   // end of this particular case
        }       // end switch(buffer)
    }           // end if(buffer[0] == ':')
    if(n <= 0) break;
  }             // end while(true) rx/tx loop
 }              // end while(true) tcp connect/disconnect loop
}               // end main

void pdm_init(){

  // enable clocks for SPI ports
  SIM_SCGC6 |= SIM_SCGC6_SPI0_MASK;
  SIM_SCGC6 |= SIM_SCGC6_SPI1_MASK;
  SIM_SCGC3 |= SIM_SCGC3_SPI2_MASK;

  // Enable clock for PortB and PortD
  SIM_SCGC5 |= SIM_SCGC5_PORTB_MASK; // SPI2
  SIM_SCGC5 |= SIM_SCGC5_PORTD_MASK; // SPI0, SPI1

  // check setting for "SMPL_PT"
  SPI1_MCR |= 1;
  SPI1_MCR |=   SPI_MCR_MSTR_MASK | SPI_MCR_CONT_SCKE_MASK | SPI_MCR_HALT_MASK |
SPI_MCR_DIS_TXF_MASK | SPI_MCR_DIS_RXF_MASK; //master mode, continuous SCK, stopped (started
after initialization), TX fifo disabled, RX fifo disabled
  SPI1_CTAR0 &= 0xfffcffff;
  //SPI1_CTAR0 = SPI_CTAR_DBR_MASK | SPI_CTAR_FMSZ(15) | SPI_CTAR_PBR(2) | SPI_CTAR_ASC(2)
| SPI_CTAR_BR(2) | SPI_CTAR_CPHA_MASK; // baud = 4Mhz, frame size = 7+1 bits, CPOL = 0, CPHA = 1,
MSB first  //0xB8020202
  //SPI1_CTAR0 = SPI_CTAR_FMSZ(15) | SPI_CTAR_PBR(2) | SPI_CTAR_ASC(3) | SPI_CTAR_BR(2) |
SPI_CTAR_CPHA_MASK; // baud = 4Mhz, frame size = 7+1 bits, CPOL = 0, CPHA = 1, MSB first
//0xB8020202
  SPI1_RSER =  SPI_RSER_RFDF_RE_MASK | SPI_RSER_RFDF_DIRS_MASK;  // enable requests, set
requests to DMA requests instead of interrupts

  // Start SPI ports
  SPI1_MCR &= ~SPI_MCR_HALT_MASK;
}
```

```
void clearBuffer() {
   for(int i = 0; i < 100; i++) buffer[i] = 0;
}


//void clearFault() {
//    for(int i = 100; i < 200; i++) buffer[i] = 0;
//}

bool syncAngles(){
   for(int i = 0; i < 10; i++){ // timeout after 10 tries
      int angle = angle_encoder.absolute_angle();
      if(angle != 0x00ff0000) {
         quad_update(angle);
         return true;
      }
   }
   return false;
}

#include "spi_api.h"
#include "cmsis.h"
#include "pinmap.h"
#include "mbed_error.h"
#include "fsl_clock_manager.h"
#include "fsl_dspi_hal.h"
#include "PeripheralPins.h"
int spi_start(){
   // wait tx buffer empty
   int timeout = 0xffff;
   while(!DSPI_HAL_GetStatusFlag(SPI1_BASE, kDspiTxFifoFillRequest) && --timeout);
   dspi_command_config_t command = {0};
   command.isEndOfQueue = true;
   command.isChipSelectContinuous = 0;
   DSPI_HAL_WriteDataMastermode(SPI1_BASE, &command, (uint16_t)0x00f0);
   DSPI_HAL_ClearStatusFlag(SPI1_BASE, kDspiTxFifoFillRequest);

   // wait rx buffer full
   timeout = 0xff;
   while (!DSPI_HAL_GetStatusFlag(SPI1_BASE, kDspiRxFifoDrainRequest) && --timeout);
   DSPI_HAL_ClearStatusFlag(SPI1_BASE, kDspiRxFifoDrainRequest);
   return DSPI_HAL_ReadData(SPI1_BASE) & 0xff;
```

MotorControl.cpp

```
#include "MotorControl.h"

#ifdef DEBUG_ON
#undef DEBUG_ON
#endif
#define DEBUG_ON 1
```

```
DigitalOut led_red(LED_RED);
DigitalOut led_green(LED_GREEN);
DigitalOut led_blue(LED_BLUE);

// angle encoder
AngleEncoder angle_encoder(PTD2, PTD3, PTD1, PTD0, 8, 0, 1000000); // mosi, miso, sclk, cs, bit_width, mode,
hz

// constructor
MotorControl::MotorControl(PinName cw, PinName ccw, int period, int safetyPeriod) :
        _cw(cw),
        _ccw(ccw) {

    // turn motor off
    _cw = 0;
    _ccw = 0;

    _cw.period_us(period);
    _ccw.period_us(period);

    _period = period;
    _safetyPeriod = safetyPeriod;

    _calibrated = false;
}

void MotorControl::calibrate(){
    off();

    maxAngle = -5000;
    minAngle = 5000;
    int pastAngle;
    int derivative;
    int currAngle = angle_encoder.absolute_angle();
    for(int i = 0; i < 150; i++){
        pastAngle = currAngle;
        currAngle = angle_encoder.absolute_angle();
        if (currAngle > 2048 || currAngle < -2048) currAngle = angle_encoder.absolute_angle();
        derivative = currAngle-pastAngle;
        if(derivative > 50) {
            printf("Dropped\r\n");
            off();
            _ccw = 0.7;
            pause_us(2000);
            off();
            pause(0.5);
        }
        if(currAngle > maxAngle && currAngle != 0x00ff0000) maxAngle = currAngle;
        if(currAngle < minAngle) minAngle = currAngle;
        printf("C: %4i\tD: %4i\tMax: %4i\tMin: %4i\r\n",currAngle,derivative,maxAngle,minAngle);
        _cw = 1;
        pause_us(2000);
        if(currAngle > 400){ // used in case the mallet is in a deep hole during calibration
            pause_us(1000); // leave the motor on for a little longer
            i -= 5;
            printf("Calibration extended\r\n");
```

```
        }
        off();
        pause_ms(40);
    }
    printf("\r\n\nMax: %i\r\nMin: %i\r\n",maxAngle,minAngle);

    for(int i = 0; i < 40; i++) calibrationVar[i] = minAngle;

    coarseThreshold = minAngle + 120;  // 50
    fallThreshold = minAngle + 220;    // 80
    fineMinThreshold = minAngle - 10;          // -10 for extra margin, more negative would mean the reset mallet is
extra high, which dirt or anything on the mallet or cam might cause.
    fineMaxThreshold = minAngle + 15;         // 12

    printf("CoarseThreshold: %i\r\n",coarseThreshold);
    printf("FallThreshold: %i\r\n",fallThreshold);
    printf("FineMinThreshold: %i\r\n",fineMinThreshold);
    printf("FineMaxThreshold: %i\r\n",fineMaxThreshold);
    // reset the mallet after calibration
    off();
    pause_ms(100);
    resetMallet();
    off();
    _calibrated = true;
}

bool MotorControl::getCalibration(){
    return _calibrated;
}

void MotorControl::releaseMallet() {
    // make sure motor is off
    off();
    //int angle;
    //int tempMinAngle = 2048;
    // pulse clockwise to release mallet
    _cw = 1;
    pause_ms(10);
    _cw = 0;
    /*
    for(int i = 0; i < 50; i++){ // pause 50 ms, max absolute read speed is 100kHz
        angle = angle_encoder.absolute_angle();
        if(angle < tempMinAngle && angle > -2048) tempMinAngle = angle;
    }*/
    pause_ms(50);

    // pulse counter-clockwise to stop snail cam
    _ccw = 0.7;
    pause_ms(5);
    _ccw = 0;

    // make sure motor is off
    off();

    //tempMinAngle -= 3; // the tempMinAngle tends to be higher than should be by 3.
    //DEBUG printf("release angle: %i\r\n", tempMinAngle);
```

```
    //if(tempMinAngle < minAngle-5 || tempMinAngle > minAngle + 5){
    //    DEBUG printf("Consider recalibrating this mallet\r\n");
    //}
}


int MotorControl::resetMallet() {

    led_red = 1;
    led_blue = 1;
    led_green = 1;

    // while loop exits when the cam as settled in the window for 5 iterations
    int set = 0;
    int coarseResetCnt = 0;
    int fineResetCnt = 0;
    while(set < 5){

        int angle = angle_encoder.absolute_angle();
        if(angle != 0x00ff0000){
            DEBUG printf("set: %i\tangle: %i\r\n",set, angle);
            // cam fell off during fineReset, so use coarseReset again
            if(angle > fallThreshold && coarseResetCnt < 4) { // angle > fallThreshold
                DEBUG printf("a\r\n");
                coarseReset();
                coarseResetCnt++;
                set = 0;
                fineResetCnt = 0;
            }

            // cam is within window, start counting iterations to make sure the cam is settled
            else if(angle <= fineMaxThreshold && angle >= fineMinThreshold) {
                set++;
                DEBUG printf("b\r\n");
            }

            // use fineReset to finish moving cam to correct spot
            else {
                DEBUG printf("c\r\n");
                int angle = fineReset();
                fineResetCnt++;
                if(fineResetCnt < 5){
                    _ccw = 0.2;
                    pause_us(_period);
                    off();
                }
                DEBUG printf("d\t angle: %i\r\n", angle_encoder.absolute_angle());
                set = 2;
            }
            pause_ms(50);
        }
    }
    DEBUG printf("e\r\n");

    off();
    led_red = 1;
```

```
    led_blue = 1;
    led_green = 1;
    return 0;
}

void MotorControl::coarseReset() {
    led_blue = 0;
    //coarseThreshold = 50;

    off();
    for(int i = 0; i < 4; i++){
        if(angle_encoder.absolute_angle() < coarseThreshold) break;
        _cw = 1;
        pause_ms(6);
        off();
        pause_ms(100);
    }
    pause_ms(100);
    off();
}

int MotorControl::fineReset() {
    led_red = 0;
    //fineMaxThreshold = 12;
    //fineMinThreshold = 0;
    //fallThreshold = 80;

    // make sure motor is off
    off();

    int angle = angle_encoder.absolute_angle();
    int pastAngle;
    int derivCnt = 0;
    bool set = false;
    double dutyCycle = 0.7;
    double maxDutyCycle = 0.80;
    double minDutyCycle = 0.50;
    while(!set){
        pastAngle = angle;
        angle = angle_encoder.absolute_angle();
            if(angle != 0x00ff0000){
            if(angle == pastAngle){
                derivCnt++;
            }
            else derivCnt = 0;

            printf("A: %i, P: %i, D: %i, F: %f\r\n",angle, pastAngle, pastAngle-angle, dutyCycle);
            if(angle > 100) maxDutyCycle = 0.68;
            if((pastAngle-angle) == 0) dutyCycle += 0.05;
            if((pastAngle-angle) > 20) dutyCycle -= 0.05;
            if(dutyCycle < minDutyCycle) dutyCycle = minDutyCycle; //minimum duty cycle
            if(dutyCycle > maxDutyCycle) dutyCycle = maxDutyCycle; // maximum duty cycle
            // cam is in the correct window, so exit loop
            if(angle <= fineMaxThreshold && angle >= fineMinThreshold) set = true;
```

```
        // cam accidentally released the mallet again, exit loop so coarse reset can occur (this is important, b/c the
fine reset will attempt to rotate ccw and will break the motor)
        /*else if(angle > fallThreshold) {
            set = true;
        }*/

        // nudge cam either cw or ccw until it is positioned within the window
        else{
            if(angle > fineMaxThreshold) _cw = dutyCycle;
            else if(angle < fineMinThreshold) { return 0; }
            pause_us(2000);
            off();
            pause_ms(10);
        }
      }
   }

   // make sure motor is off
   off();
   return angle_encoder.absolute_angle();
}

void MotorControl::off() {
   _cw = 0;
   _ccw = 0;
   pause_us(_safetyPeriod);
}

/*
void MotorControl::clockwise(float dutyCycle) {
   _ccw = 0;
   _cw = dutyCycle;
}*/
```

pdb.cpp

```
#include "pdb.h"
#include "dma.h"


DigitalOut toggle_pdb(PTB23);


/*  The PDB is setup to run continuous (when enabled) so it will
 *  periodically trigger the ADCs to sample and trigger DMA2 to
 *  save the quadrature angle.  The PDB can be started and stopped. */
void pdb_init() {

   // initialize the Programmable Delay Block

   // turn on the clock to the PDB
   SIM->SCGC6 |= SIM_SCGC6_PDB_MASK;
```

```
    // set ADC trigger to PDB0
    SIM_SOPT7 = SIM_SOPT7_ADC0TRGSEL(0);

    // input frequency is 6 Mhz?
    // Configure the Peripheral Delay Block (PDB):
    //#define SLOW
    #ifdef SLOW
    PDB0_IDLY = 0;   // need to trigger interrupt every counter reset which happens when modulus reached
    PDB0_MOD = 0xffff;//0x257; // period of timer set to 10us
    PDB0_CH0DLY0 = 0;
    PDB0_CH0DLY1 = 0;
    PDB0_CH1DLY0 = 0;
    PDB0_CH1DLY1 = 0;
    PDB0_CH0C1 = PDB_C1_EN(2) | PDB_C1_TOS(2); // channel 0 pretrigger 0 and 1 enabled and delayed
    PDB0_CH1C1 = PDB_C1_EN(1) | PDB_C1_TOS(1); // channel 1 pretrigger 0 and 1 enabled and delayed

    // Setup Staus and Control Register
    PDB0_SC = 0; // clear register
    PDB0_SC = PDB_SC_DMAEN_MASK    // Enable DMA
            | PDB_SC_PRESCALER(5) // Slow down the period of the PDB for testing
            | PDB_SC_TRGSEL(0xf)  // Trigger source is Software Trigger to be invoked in this file
            | PDB_SC_PDBEN_MASK   // PDB enabled
            | PDB_SC_PDBIE_MASK   // PDB Interrupt Enable
            | PDB_SC_MULT(1)      // Multiplication factor
            | PDB_SC_CONT_MASK    // Contintuous, rather than one-shot, mode
            | PDB_SC_LDOK_MASK;   // Need to ok the loading or it will not load certain regsiters!
    #else
    PDB0_IDLY = 0;   // need to trigger interrupt every counter reset which happens when modulus reached
    PDB0_MOD = 0x257; // period of timer set to 10us
    PDB0_CH0DLY0 = 0;
    PDB0_CH0DLY1 = 0;
    PDB0_CH1DLY0 = 0;
    PDB0_CH1DLY1 = 0;
    PDB0_CH0C1 = PDB_C1_EN(2) | PDB_C1_TOS(2); // channel 0 pretrigger 0 and 1 enabled and delayed
    PDB0_CH1C1 = PDB_C1_EN(1) | PDB_C1_TOS(1); // channel 1 pretrigger 0 and 1 enabled and delayed

    // Setup Staus and Control Register
    PDB0_SC = 0; // clear register
    PDB0_SC = PDB_SC_DMAEN_MASK    // Enable DMA
            | PDB_SC_PRESCALER(1) // Slow down the period of the PDB for testing
            | PDB_SC_TRGSEL(0xf)  // Trigger source is Software Trigger to be invoked in this file
            | PDB_SC_PDBEN_MASK   // PDB enabled
            | PDB_SC_PDBIE_MASK   // PDB Interrupt Enable
            | PDB_SC_MULT(0)      // Multiplication factor
            | PDB_SC_CONT_MASK    // Contintuous, rather than one-shot, mode
            | PDB_SC_LDOK_MASK;   // Need to ok the loading or it will not load certain regsiters!
    #endif

}

void pdb_start() {
    dma_reset();
    PDB0_SC |= PDB_SC_PDBEN_MASK;  // PDB enabled
    PDB0_SC |= PDB_SC_SWTRIG_MASK; // enable software trigger (start the PDB)
}
```

```
void pdb_stop() {
   PDB0_SC &= ~PDB_SC_PDBEN_MASK;  // PDB disabled
}

/* * * * * * * * * * * * * * * For Debugging Purposes * * * * * * * * * * * * * * * * * * * * * * */

// Enables the interrupt for PDB0, which toggles PTB23.
// Scope PTB23 to verify the frequency.
void pdb_enable_interrupt() {
   PDB0_SC &= ~PDB_SC_DMAEN_MASK; // disable DMA, this stops DMA2 from functioning
   NVIC_SetVector(PDB0_IRQn, (uint32_t)&PDB0_IRQHandler);
   NVIC_EnableIRQ(PDB0_IRQn);
}
void pdb_disable_interrupt() {
   NVIC_DisableIRQ(PDB0_IRQn); // disable interrupt
   PDB0_SC |= PDB_SC_DMAEN_MASK; // enable DMA (this lets DMA2 function)
}
void PDB0_IRQHandler() {
   toggle_pdb = !toggle_pdb;
   PDB0_SC &= ~PDB_SC_PDBIF_MASK; // clear interrupt flag
}

void pdb_print_registers() {
   Serial debug2(USBTX,USBRX);
   debug2.printf("PDB0_SC:       %08x\r\n",PDB0_SC);
   debug2.printf("PDB0_MOD:      %08x\r\n",PDB0_MOD);
   debug2.printf("PDB0_CNT:      %08x\r\n",PDB0_CNT);
   debug2.printf("PDB0_IDLY:     %08x\r\n",PDB0_IDLY);
   debug2.printf("PDB0_CH0C1:    %08x\r\n",PDB0_CH0C1);
   debug2.printf("PDB0_CH0S:     %08x\r\n",PDB0_CH0S);
   debug2.printf("PDB0_CH0DLY0:  %08x\r\n",PDB0_CH0DLY0);
   debug2.printf("PDB0_CH0DLY1:  %08x\r\n",PDB0_CH0DLY1);
   debug2.printf("PDB0_CH1C1:    %08x\r\n",PDB0_CH1C1);
   debug2.printf("PDB0_CH1S:     %08x\r\n",PDB0_CH1S);
   debug2.printf("PDB0_CH1DLY0:  %08x\r\n",PDB0_CH1DLY0);
   debug2.printf("PDB0_CH1DLY1:  %08x\r\n",PDB0_CH1DLY1);
   debug2.printf("PDB0_DACINTC0: %08x\r\n",PDB0_DACINTC0);
   debug2.printf("PDB0_DACINT0:  %08x\r\n",PDB0_DACINT0);
   debug2.printf("PDB0_DACINTC1: %08x\r\n",PDB0_DACINTC1);
   debug2.printf("PDB0_DACINT1:  %08x\r\n",PDB0_DACINT1);
   debug2.printf("PDB0_POEN:     %08x\r\n",PDB0_POEN);
   debug2.printf("PDB0_PO0DLY:   %08x\r\n",PDB0_PO0DLY);
   debug2.printf("PDB0_PO1DLY:   %08x\r\n",PDB0_PO1DLY);
   debug2.printf("PDB0_PO2DLY:   %08x\r\n\n",PDB0_PO2DLY);
}
```

dma.cpp

```
/**
 *  Setup triggering for DMA2 and PortC
 */
```

```
#include "dma.h"

DigitalOut toggle_dma0(LED_RED);
DigitalOut toggle_dma1(LED_BLUE);
DigitalOut toggle_dma2(LED_GREEN);
Serial debug3(USBTX,USBRX);

int len_mic = TOTAL_SAMPLES_MIC;
int len_angle = TOTAL_SAMPLES_ANGLE;
uint16_t sample_array0[TOTAL_SAMPLES_MIC];
#ifndef MEMS
uint16_t sample_array1[TOTAL_SAMPLES_MIC];
#endif
uint16_t angle_array[TOTAL_SAMPLES_ANGLE];
bool dma_done = false;
bool dma_half_done = false;
uint32_t transmit_command = 0x80010000;


/*
 *
 *   */
#ifdef MEMS
void dma_spi_init()
{
   debug3.baud(230400);

   toggle_dma0 = 1;
   toggle_dma1 = 1;
   // Enable clock for DMAMUX and DMA
   SIM_SCGC6 |= SIM_SCGC6_DMAMUX_MASK | SIM_SCGC6_SPI1_MASK;
   SIM_SCGC7 |= SIM_SCGC7_DMA_MASK;
   SIM_SCGC6 |= SIM_SCGC6_FTM2_MASK; // make sure clock is enabled for FTM2
   // SIM_SCGC3 = SPI2
   // SIM_SCGC6 = SPI0, SPI1, DMAMUX
   // SIM_SCGC7 = DMA


   // Enable DMA channels and select MUX to the correct source (see page 95 of user manual)
   // DMA0 reads from SPI1
   // DMA1 does nothing, but can be used for a second microphone in the future if needs be
   // DMA2 samples the FTM module (angle encoder)
   // DMA3 writes to SPI1 to make it transmit, which also makes it receive data, which is recorded by DMA0
   DMAMUX_CHCFG0 |= DMAMUX_CHCFG_ENBL_MASK | DMAMUX_CHCFG_SOURCE(16); // SPI1
   //DMAMUX_CHCFG1 |= DMAMUX_CHCFG_ENBL_MASK | DMAMUX_CHCFG_SOURCE(17); // SPI2
   DMAMUX_CHCFG2 |= DMAMUX_CHCFG_ENBL_MASK | DMAMUX_CHCFG_SOURCE(48); // Set
trigger source to PDB (Don't set DMA Trig Enable because that is for the PIT)
   DMAMUX_CHCFG3 |= DMAMUX_CHCFG_ENBL_MASK | DMAMUX_CHCFG_SOURCE(16); // DMA to
transmit to SPI1
   /*
   Source   Number (Page 95 of User Manual)
   spi0_rx  14
   spi0_tx  15
   spi1     16
   spi2     17
   */
```

```
    // Enable request signal for channel 0
    DMA_ERQ = DMA_ERQ_ERQ0_MASK | DMA_ERQ_ERQ2_MASK | DMA_ERQ_ERQ3_MASK;

    // select round-robin arbitration priority
    //DMA_CR |= DMA_CR_ERCA_MASK;

    // Set memory address for source and destination for DMA0, DMA2, and DMA3
    DMA_TCD0_SADDR = (uint32_t) &SPI1_POPR;
    DMA_TCD0_DADDR = (uint32_t) sample_array0;
    //DMA_TCD1_SADDR = (uint32_t) &SPI1_RXFR2;
    //DMA_TCD1_DADDR = (uint32_t) sample_array1;
    DMA_TCD2_SADDR = (uint32_t) &FTM2_CNT;
    DMA_TCD2_DADDR = (uint32_t) angle_array;
    DMA_TCD3_SADDR = (uint32_t) &transmit_command;
    DMA_TCD3_DADDR = (uint32_t) &SPI1_PUSHR;

    // Set an offset for source and destination address
    DMA_TCD0_SOFF = 0x00; // Source address offset of 0 bits per transaction
    DMA_TCD0_DOFF = 0x02; // Destination address offset of 2 bit per transaction (2 bytes)
    //DMA_TCD1_SOFF = 0x00; // Source address offset of 0 bits per transaction
    //DMA_TCD1_DOFF = 0x02; // Destination address offset of 2 bit per transaction
    DMA_TCD2_SOFF = 0x00; // Source address offset of 0 bits per transaction
    DMA_TCD2_DOFF = 0x02; // Destination address offset of 2 bit per transaction
    DMA_TCD3_SOFF = 0;
    DMA_TCD3_DOFF = 0;

    // Set source and destination data transfer size
    DMA_TCD0_ATTR = DMA_ATTR_SSIZE(1) | DMA_ATTR_DSIZE(1);
    //DMA_TCD1_ATTR = DMA_ATTR_SSIZE(1) | DMA_ATTR_DSIZE(1);
    DMA_TCD2_ATTR = DMA_ATTR_SSIZE(1) | DMA_ATTR_DSIZE(1);
    DMA_TCD3_ATTR = DMA_ATTR_SSIZE(2) | DMA_ATTR_DSIZE(2);

    // Number of bytes to be transfered in each service request of the channel
    DMA_TCD0_NBYTES_MLNO = 0x02;
    //DMA_TCD1_NBYTES_MLNO = 0x02;
    DMA_TCD2_NBYTES_MLNO = 0x02;
    DMA_TCD3_NBYTES_MLNO = 0x04;

    // Current major iteration count
    DMA_TCD0_CITER_ELINKNO = DMA_CITER_ELINKNO_CITER(len_mic);
    DMA_TCD0_BITER_ELINKNO = DMA_BITER_ELINKNO_BITER(len_mic);
    //DMA_TCD1_CITER_ELINKNO = DMA_CITER_ELINKNO_CITER(len_mic);
    //DMA_TCD1_BITER_ELINKNO = DMA_BITER_ELINKNO_BITER(len_mic);
    DMA_TCD2_CITER_ELINKNO = DMA_CITER_ELINKNO_CITER(len_angle);
    DMA_TCD2_BITER_ELINKNO = DMA_BITER_ELINKNO_BITER(len_angle);
    DMA_TCD3_CITER_ELINKNO = DMA_CITER_ELINKNO_CITER(len_mic);
    DMA_TCD3_BITER_ELINKNO = DMA_BITER_ELINKNO_BITER(len_mic);


    // Adjustment value used to restore the source and destination address to the initial value
    // After reading 'len' number of times, the DMA goes back to the beginning by subtracting len*2 from the address
(going back to the original address)

    DMA_TCD0_SLAST = 0;      // Source address adjustment
    DMA_TCD0_DLASTSGA = -len_mic*2;  // Destination address adjustment
```

```
    //DMA_TCD1_SLAST = 0;      // Source address adjustment
    //DMA_TCD1_DLASTSGA = -len_mic*2;  // Destination address adjustment
    DMA_TCD2_SLAST = 0;      // Source address adjustment
    DMA_TCD2_DLASTSGA = -len_angle*2;  // Destination address adjustment
    DMA_TCD3_SLAST = 0;
    DMA_TCD3_DLASTSGA = 0;

    // Setup control and status register
    DMA_TCD0_CSR = 0;
    //DMA_TCD1_CSR = 0;
    DMA_TCD2_CSR = 0;
    DMA_TCD3_CSR = 0;

    // enable interrupt call at end of major loop
    DMA_TCD0_CSR |= DMA_CSR_INTMAJOR_MASK | DMA_CSR_INTHALF_MASK;
    //DMA_TCD1_CSR |= DMA_CSR_INTMAJOR_MASK | DMA_CSR_INTHALF_MASK;
    DMA_TCD2_CSR |= DMA_CSR_INTMAJOR_MASK;
    DMA_TCD3_CSR |= DMA_CSR_INTMAJOR_MASK | DMA_CSR_INTHALF_MASK;

    // add interrupt handlers to interrupt vector table
    NVIC_SetVector(DMA0_IRQn, (uint32_t)&DMA0_IRQHandler);
    //NVIC_SetVector(DMA1_IRQn, (uint32_t)&DMA1_IRQHandler);
    NVIC_SetVector(DMA2_IRQn, (uint32_t)&DMA2_IRQHandler);
    //NVIC_SetVector(DMA3_IRQn, (uint32_t)&DMA3_IRQHandler);

    // make sure all interrupt flags are cleared
    DMA_CINT = DMA_CINT_CAIR_MASK;

    //enable interrupts
    NVIC_EnableIRQ(DMA0_IRQn);
    //NVIC_EnableIRQ(DMA1_IRQn);
    NVIC_EnableIRQ(DMA2_IRQn);
    //NVIC_EnableIRQ(DMA3_IRQn);
}


/*  DMA0 and DMA1 are triggered by ADC0 and ADC1 (which are triggered
 *  by the PDB).  However, DMA2 is triggered directly by the PDB.  This
 *  is becuase DMA2 is reading FTM2, which cannot trigger the DMA.   */
#else
void dma_adc_init()
{
    toggle_dma0 = 1;
    toggle_dma1 = 1;
    toggle_dma2 = 1;
    // Enable clock for DMAMUX and DMA
    SIM_SCGC6 |= SIM_SCGC6_DMAMUX_MASK;
    SIM_SCGC7 |= SIM_SCGC7_DMA_MASK;
    SIM_SCGC6 |= SIM_SCGC6_FTM2_MASK; // make sure clock is enabled for FTM2

    // Enable DMA channels and select MUX to the correct source (see page 95 of user manual
    DMAMUX_CHCFG0 |= DMAMUX_CHCFG_ENBL_MASK | DMAMUX_CHCFG_SOURCE(40); // ADC0
    DMAMUX_CHCFG1 |= DMAMUX_CHCFG_ENBL_MASK | DMAMUX_CHCFG_SOURCE(41); // ADC1
    DMAMUX_CHCFG2 |= DMAMUX_CHCFG_ENBL_MASK | DMAMUX_CHCFG_SOURCE(48); // Set
trigger source to PDB (Don't set DMA Trig Enable because that is for the PIT)
    /* Source number    Source module
```

```
    40          ADC0
    41          ADC1
    48          PDB
*/


  // Enable request signal for channel 0
  DMA_ERQ = DMA_ERQ_ERQ0_MASK | DMA_ERQ_ERQ1_MASK | DMA_ERQ_ERQ2_MASK;

  // select round-robin arbitration priority
  DMA_CR |= DMA_CR_ERCA_MASK;

  // Set memory address for source and destination for DMA0, DMA1, and DMA2
  DMA_TCD0_SADDR = (uint32_t) &ADC0_RB;
  DMA_TCD0_DADDR = (uint32_t) sample_array0;
  DMA_TCD1_SADDR = (uint32_t) &ADC1_RA;
  DMA_TCD1_DADDR = (uint32_t) sample_array1;
  DMA_TCD2_SADDR = (uint32_t) &FTM2_CNT;
  DMA_TCD2_DADDR = (uint32_t) angle_array;

  // Set an offset for source and destination address
  DMA_TCD0_SOFF = 0x00; // Source address offset of 2 bits per transaction
  DMA_TCD0_DOFF = 0x02; // Destination address offset of 1 bit per transaction
  DMA_TCD1_SOFF = 0x00; // Source address offset of 2 bits per transaction
  DMA_TCD1_DOFF = 0x02; // Destination address offset of 1 bit per transaction
  DMA_TCD2_SOFF = 0x00; // Source address offset of 2 bits per transaction
  DMA_TCD2_DOFF = 0x02; // Destination address offset of 1 bit per transaction

  // Set source and destination data transfer size
  DMA_TCD0_ATTR = DMA_ATTR_SSIZE(1) | DMA_ATTR_DSIZE(1);
  DMA_TCD1_ATTR = DMA_ATTR_SSIZE(1) | DMA_ATTR_DSIZE(1);
  DMA_TCD2_ATTR = DMA_ATTR_SSIZE(1) | DMA_ATTR_DSIZE(1);

  // Number of bytes to be transfered in each service request of the channel
  DMA_TCD0_NBYTES_MLNO = 0x02;
  DMA_TCD1_NBYTES_MLNO = 0x02;
  DMA_TCD2_NBYTES_MLNO = 0x02;

  // Current major iteration count
  DMA_TCD0_CITER_ELINKNO = DMA_CITER_ELINKNO_CITER(len_mic);
  DMA_TCD0_BITER_ELINKNO = DMA_BITER_ELINKNO_BITER(len_mic);
  DMA_TCD1_CITER_ELINKNO = DMA_CITER_ELINKNO_CITER(len_mic);
  DMA_TCD1_BITER_ELINKNO = DMA_BITER_ELINKNO_BITER(len_mic);
  DMA_TCD2_CITER_ELINKNO = DMA_CITER_ELINKNO_CITER(len_angle);
  DMA_TCD2_BITER_ELINKNO = DMA_BITER_ELINKNO_BITER(len_angle);

  // Adjustment value used to restore the source and destiny address to the initial value
  // After reading 'len' number of times, the DMA goes back to the beginning by subtracting len*2 from the address
(going back to the original address)

  DMA_TCD0_SLAST = 0;      // Source address adjustment
  DMA_TCD0_DLASTSGA = -len_mic*2;  // Destination address adjustment
  DMA_TCD1_SLAST = 0;      // Source address adjustment
  DMA_TCD1_DLASTSGA = -len_mic*2;  // Destination address adjustment
  DMA_TCD2_SLAST = 0;      // Source address adjustment
  DMA_TCD2_DLASTSGA = -len_angle*2;  // Destination address adjustment
```

```
    // Setup control and status register
    DMA_TCD0_CSR = 0;
    DMA_TCD1_CSR = 0;
    DMA_TCD2_CSR = 0;

    // enable interrupt call at end of major loop
    //DMA_TCD0_CSR |= DMA_CSR_INTMAJOR_MASK | DMA_CSR_INTHALF_MASK;
    DMA_TCD0_CSR |= DMA_CSR_INTMAJOR_MASK;

    // add interrupt handlers to interrupt vector table
    NVIC_SetVector(DMA0_IRQn, (uint32_t)&DMA_IRQHandler);

    //enable interrupts
    NVIC_EnableIRQ(DMA0_IRQn);

    // dma_init takes 4.09us to run.
}
#endif

void dma_reset() {
    dma_done = false;
    dma_half_done = false;

    // clear all DMA interrupts
    DMA_CINT = DMA_CINT_CAIR_MASK;

    DMA_ERQ |= DMA_ERQ_ERQ3_MASK;

    //enable interrupts
    NVIC_EnableIRQ(DMA0_IRQn);
    NVIC_EnableIRQ(DMA2_IRQn);
}

/* The only DMA interrupt is from DMA0.  The interrupts from DMA1 and DMA2
 * are turned off because they all trigger at the same time.  Actually
 * DMA2 triggers just before DMA0 and DMA1, but it's a negligible amount
 * of time.  By the time the PDB is turned off, the ADCs will have already
 * been triggered.  */
void DMA0_IRQHandler() {

    DMA_CINT |= DMA_CINT_CINT(0); // clear interrupt flag
    if(!dma_half_done) {
        dma_half_done = true;
        //debug3.printf("half done\r\n");
        return;
    }
    //PDB0_SC &= ~PDB_SC_PDBEN_MASK;  // disable PDB
    NVIC_DisableIRQ(DMA0_IRQn); // disable interrupt
    dma_done = true;
    DMA_ERQ &= ~DMA_ERQ_ERQ3_MASK;
    //debug3.printf("DMA0 done\r\n");
}

void DMA2_IRQHandler() {
```

```
    DMA_CINT |= DMA_CINT_CINT(2); // clear DMA2 interrupt flag
    PDB0_SC &= ~PDB_SC_PDBEN_MASK;  // disable PDB
    NVIC_DisableIRQ(DMA2_IRQn); // disable DMA2 interrupt
    //debug3.printf("DMA2 done\r\n");
}


/* * * * * * * * * * * * * * For Debugging Purposes * * * * * * * * * * * * * * * * * * * * * */


void dma_print_registers() {

    debug3.printf("SADDR0: 0x%08x\r\n",DMA_TCD0_SADDR);
    debug3.printf("DADDR0: 0x%08x\r\n",DMA_TCD0_DADDR);
    debug3.printf("SADDR1: 0x%08x\r\n",DMA_TCD1_SADDR);
    debug3.printf("DADDR1: 0x%08x\r\n",DMA_TCD1_DADDR);
    debug3.printf("SADDR2: 0x%08x\r\n",DMA_TCD2_SADDR);
    debug3.printf("DADDR2: 0x%08x\r\n",DMA_TCD2_DADDR);

    debug3.printf("CITER0: 0x%08x\r\n",DMA_TCD0_CITER_ELINKNO);
    debug3.printf("BITER0: 0x%08x\r\n",DMA_TCD0_BITER_ELINKNO);
    debug3.printf("CITER1: 0x%08x\r\n",DMA_TCD1_CITER_ELINKNO);
    debug3.printf("BITER1: 0x%08x\r\n",DMA_TCD1_BITER_ELINKNO);
    debug3.printf("CITER2: 0x%08x\r\n",DMA_TCD2_CITER_ELINKNO);
    debug3.printf("BITER2: 0x%08x\r\n",DMA_TCD2_BITER_ELINKNO);


    debug3.printf("DMA_CR: %08x\r\n", DMA_CR);
    debug3.printf("DMA_ES: %08x\r\n", DMA_ES);
    debug3.printf("DMA_ERQ: %08x\r\n", DMA_ERQ);
    debug3.printf("DMA_EEI: %08x\r\n", DMA_EEI);
    debug3.printf("DMA_CEEI: %02x\r\n", DMA_CEEI);
    debug3.printf("DMA_SEEI: %02x\r\n", DMA_SEEI);
    debug3.printf("DMA_CERQ: %02x\r\n", DMA_CERQ);
    debug3.printf("DMA_SERQ: %02x\r\n", DMA_SERQ);
    debug3.printf("DMA_CDNE: %02x\r\n", DMA_CDNE);
    debug3.printf("DMA_SSRT: %02x\r\n", DMA_SSRT);
    debug3.printf("DMA_CERR: %02x\r\n", DMA_CERR);
    debug3.printf("DMA_CINT: %02x\r\n", DMA_CINT);
    debug3.printf("DMA_INT: %08x\r\n", DMA_INT);
    debug3.printf("DMA_ERR: %08x\r\n", DMA_ERR);
    debug3.printf("DMA_HRS: %08x\r\n", DMA_HRS);
}
```

Python 2.7 Code for running the analysis of the impact audio data and obtaining BAE values for each impact

```
import sys
import os, os.path, fnmatch
import numpy as np, pylab, scipy
import time
import Tkinter, tkFileDialog
import functions as func
```

```
import csv
from collections import defaultdict

start = time.clock()

FILETYPE = '.txt'

rootDir = "../DataFiles"

def runAnalysis1(rootDir):
    analysisDir = rootDir + 'Analysis'
    malletdirList = []
    print analysisDir
    # if analysis directory doesn't exist, create it
    if not os.path.exists(analysisDir):
        os.makedirs(analysisDir)
        print 'Analysis directory created'

    # get list of all the mallets
    malletdirList = os.listdir(rootDir)
    for d in malletdirList:
        if not os.path.isdir(rootDir + d):
            malletdirList.remove(d)

    if 'Analysis' in malletdirList: malletdirList.remove('Analysis')
    else: print 'Analysis directory not found'

    if len(malletdirList) == 0: return # no mallet folders, so return
    fileCnt = 0
    for subDir in malletdirList:
        currDir = rootDir + subDir
        if os.path.isdir(currDir):
            fileList = os.listdir(currDir)
            fileCnt += len(fileList)
    if fileCnt == 0: return #no impacts within the mallet folders, so return

#find the minimum distance (actually finds min value in timestamps of the impact file names) among the mallets
#in this scan file
    distanceOffset = float("inf") #an arbitrary large number
    for subDir in malletdirList:
        currDir = rootDir + subDir
        if os.path.isdir(currDir):
            fileList = os.listdir(currDir)
            if len(fileList) > 0:
                minDistance = float(fileList[0][4:16])
                #print minDistance
                if minDistance < distanceOffset:
                    distanceOffset = minDistance
    #print 'Min Distance Test:',distanceOffset #minimum distance recorded by DMI

    # get bridge deck name and timestamp from directory name
    if rootDir[len(rootDir)-1] == '\\' or rootDir[len(rootDir)-1] == '/':
        rootDir = rootDir[0:len(rootDir)-1] #remove the slash at the end
    deckStartTime = os.path.split(rootDir)[1] #the folder at the end of the directory is the
'optionalIdentifier__startTime'
    deckName = os.path.split(os.path.split(rootDir)[0])[1] #the folder second from the end is the 'deckName'
```

```
    #create analysis file in 'Analysis' folder
    f = open(analysisDir + '/Analysis__' + deckName + '__' + deckStartTime + '.txt','w')

    # traverse subfolders analyzing the files and writing to analysis file
    rootDir = rootDir + '/'

    minMallet = int(malletdirList[0][1])
    maxMallet = int(malletdirList[len(malletdirList)-1][1])
    print '\n\n'
    print '         y'
    print '         ^'
    print '         |'
    print '         |'

    for x in range(1,8): #7 is the max number of mallets
            #first line
            if x == maxMallet: print ' mallet ---  ',
            else:              print '         |   ',

            if x < minMallet or x > maxMallet: print '|-------|',
            else:                              print '|M{0:d}-----|'.format(x),

            if x < 2 or x > 5: print ''
            else:              print '|'

            #second line
            if x == maxMallet: print 'position |   ',
            else:              print '         |   ',

            if x == 1 or x == 5:   print '  #   #    '
            elif x == 2 or x == 4: print '|       |#|'
            elif x == 3:           print '|       | |===='
            elif x == 6:           print '|       |'
            else:                  print ''
    print '         |'
    print '         +----|----------------> x '
    print '           start'
    print '          distance'
    print ''

    print rootDir
    print "Number of mallets: ", len(malletdirList)
    print 'DeckName:', deckName
    print 'StartTime:',deckStartTime
    startDistance = raw_input('Enter start distance in DMI ticks (usually 0):')
    startDistance = float(startDistance)# - distanceOffset #distanceOffset compensates for the DMI not starting at
exactly 0
    startPosition = raw_input('Enter rightmost mallet start position (distance) in feet:')
    startPosition = float(startPosition)
    direction = raw_input('Increase or decreasing?:')
    direction = direction.lower()

    #this assumes the mallets sampling are neighboring
    numMallets = len(malletdirList)
    offset = maxMallet
```

```
    if direction == 'increasing' or direction == 'i':
        direction = 1.0
    elif direction == 'decreasing' or direction == 'd':
        direction = -1.0
    else:
        direction = 1.0
        print 'Unrecognized input.  Assuming direction is increasing'

    minXpos = float("inf")  # a ridiculously large number that will undoubtedly be replaced by the actual minimum
value
    maxXpos = -float("inf") # a ridiculously small number that will undoubtedly be replaced by the actual maximum
value
    for subDir in malletdirList:
        currDir = rootDir + subDir
        fileList = os.listdir(currDir)
        if direction == -1.0: fileList = reversed(fileList)
        for filename in fileList: #go through file in increasing direction, analyzing each one
            marker1 = filename.find('__')
            if marker1 == -1 or filename[-4:] != FILETYPE: print filename, ': improper file name format'
            #elif (filename.find(subDir) == -1):print filename, ': wrong mallet name'
            else:
                filename_timestamp = float(filename[marker1+2:-4]) #get timestamp from the filename
                filename_timestamp = '{0:12.3f}'.format(filename_timestamp)
                y = (2*(offset - int(subDir[1]) ))*direction+startPosition #distance from parapet wall
                x = float("inf") #set x to something recognizeable.  it should be replaced with an actual value from the
DMI file

                #search DMI file for distance along bridge
                g = open(rootDir + 'DMI_File.txt')
                for line in g:
                    timeStamp = line[0:12]
                    if filename_timestamp == timeStamp:
                        x = float(line[13:23])
                        break
                g.close()

                x = x+startDistance
                #x = float(filename[marker1+2:marker2])*direction+startDistance

                indicators = func.analyzeFile(currDir + '\\' + filename)

                #replace 'blah' with 'indicators[2]' and delete the if/else statement
                if indicators[3] == 4095:
                    blah = 0
                    print '*'
                else: blah = indicators[3]
                print '.',
                #print "{0:11.6f} {1:11.6f} {2:14.6f} {3:11.6f} {4:11.6f} {5:11.6f} {6:11.6f}\r\n".format(x,
y,indicators[0], indicators[1], indicators[2], blah, indicators[4])
                f.write("{0:f} {1:f} {2:f} {3:f} {4:f} {5:f} {6:f}\r".format(x, y,indicators[0], indicators[1],
float(filename_timestamp), blah, indicators[4]))
                #f.write("{0:11.6f} {1:11.6f} {2:14.6f} {3:11.6f} {4:11.6f} {5:11.6f} {6:11.6f}\r".format(x,
y,indicators[0], indicators[1], indicators[2], blah, indicators[4]))
                    #x_coord  y_coord delam_index wave_speed recoilHeight bounceTime
```

```
            #print 'File:', filename, 'Y:', y, 'X:', x, 'Time:', float(filename_timestamp), 'Analysis:', indicators[0]
            #wait = raw_input("Press <RETURN> key.")

            #keep track of min and max distances
            if x > maxXpos: maxXpos = x
            if x < minXpos: minXpos = x

    f.close()
    print ''
    print 'Min Distance:', minXpos
    print 'Max Distance:', maxXpos

    print 'Mallet Distance   DelamIndex, WaveSpeed, RecoilHeight BounceTime'
    print "Run time: ", (time.clock()-start)/60.0,'min'


########start of execution of program#########

root = Tkinter.Tk()
root.withdraw()
rootDir = tkFileDialog.askdirectory(parent=root,initialdir=rootDir,title='Please select a scan folder')

if rootDir == '': exit()
#rootDir = 'C:/Users/Joe/Desktop/TraverseTek/DataFiles/a_test/a__2016-03-03__08.49AM' #jkl;

#scan the selected directory for all log.txt files (because there is one log file per scan folder)
match = []
for root, dirnames, filenames in os.walk(rootDir):
  for filename in fnmatch.filter(filenames, 'log.txt'):
    match.append(root)

for i in match:
    if i[len(i)-len('Analysis'):len(i)] == 'Analysis':# go back one directory
        dir = i[0:len(i)-len('Analysis')]
        runAnalysis1(dir)
        print '\r\n\n\n\n\n\n'

#create a combined analysis file in root folder
match = []
for root, dirnames, filenames in os.walk(rootDir):
    for filename in fnmatch.filter(filenames, 'Analysis*.txt'):
        match.append(os.path.join(root,filename))

#open all the analysis files
mapVar = []
for path in match:
    csv.register_dialect('space_delimited', delimiter=' ', skipinitialspace=True, quoting=csv.QUOTE_MINIMAL)
    alist = []
    with open(path, 'rU') as f:
        reader = csv.reader(f,'space_delimited')
        for row in reader:
            alist.append([float(a) for a in row])
    map_data=np.array(alist)
    mapVar.append(map_data)

#create a set of all the channel distances
```

```
channelSet = set()
for singleMap in mapVar:
    channelSet = channelSet | set(singleMap[:,1])

#separate the maps by channels
channels = []
for setVal in channelSet:
    #print 'CurrChannel:',setVal
    channels.append([])
    for mapNum in range(len(mapVar)): #iterate through the maps
        for rowNum in range(len(mapVar[mapNum])): #iterate through the rows
            if mapVar[mapNum][rowNum][1] == setVal:
                #print 'add',mapVar[mapNum][rowNum][1]
                channels[-1].append(mapVar[mapNum][rowNum])

#for x in range(len(channels)):
#    print [column[1] for column in channels[x]]

combinedAnalysisFilename = rootDir + '_map.txt'
print combinedAnalysisFilename

f = open(combinedAnalysisFilename,'w')
for x in range(len(channels)):
    for y in range(len(channels[x])):
        #print channels[x][y]
        f.write('{0:11.6f} {1:11.6f} {2:11.6f} {3:11.6f} {4:11.6f} {5:11.6f} {6:11.6f}\r'.format(channels[x][y][0],
channels[x][y][1], channels[x][y][2], channels[x][y][3], channels[x][y][4], channels[x][y][5], channels[x][y][6]))

f.close()
exit()
```

Python 2.7 Code for plotting the impacts and their BAE values into a delamination map

```
import csv
import operator
from collections import defaultdict
import mpl_toolkits
import Tkinter, tkFileDialog
from matplotlib.mlab import griddata
import matplotlib.patches as mpatches
import matplotlib.pyplot as plt
import matplotlib.colors as mcolors
import numpy as np
import time
import scipy.signal as sp

def import_map(filename):
    csv.register_dialect('space_delimited', delimiter=' ', skipinitialspace=True, quoting=csv.QUOTE_MINIMAL)
    alist = []
    with open(filename, 'rU') as f:
        reader = csv.reader(f,'space_delimited')
        for row in reader:
            alist.append([float(a) for a in row])
```

```
    map_data=np.array(alist)

    #average duplicate enteries
    #find duplicate distances
    DupY = defaultdict(list)
    for i,item in enumerate(map_data[:,1]):
        DupY[item].append(i)
    DupY = {k:v for k,v in DupY.items() if len(v)>1}
    #print '1',DupY

    #find duplicate mallets within duplicate distances
    for i in DupY.iterkeys():
        DupX = defaultdict(list)
        for r,item in enumerate(map_data[DupY[i],0]):
            DupX[item].append(r)
            #print '2',DupY[i][r]
        DupX = {k:v for k,v in DupX.items() if len(v)>1}
        #average the enteries that contain both a duplicate distance and mallet
        #print '****3',DupX
        for j in DupX.iterkeys():
            tempVar = np.zeros(len(map_data[0]))
            tempVar1 = np.zeros(len(map_data[0]))
            for m in range(len(DupX[j])):
                #print '\t',DupX[j][m]
                #print '\tA',DupY[i][DupX[j][m]]
                #print '\t\t',map_data[DupY[i][DupX[j][m]]]
                tempVar += map_data[DupY[i][DupX[j][m]]]
                if m == (len(DupX[j])-1):
                    tempVar1 = map_data[DupY[i][DupX[j][m]]][4] #Holds onto last timestamp occurence of duplicates
                map_data[DupY[i][DupX[j][m]]] = np.zeros(len(map_data[0]))
            tempVar = tempVar/len(DupX[j])
            map_data[DupY[i][DupX[j][m]]] = tempVar
            #print map_data[DupY[i][DupX[j][m]]]
            map_data[DupY[i][DupX[j][m]]][4] = tempVar1 #Avoids averaging for timestamp and instead saves the last
timestamp amongst the duplicate distances
            #print map_data[DupY[i][DupX[j][m]]]
            #print '\n'

    # average the duplicates
    length = len(map_data)
    cnt = 0
    while cnt < length:
        if(map_data[cnt] == np.zeros(len(map_data[0]))).all():
            map_data = np.delete(map_data,cnt,axis=0)
            cnt = cnt - 1
        cnt = cnt + 1
        length = len(map_data)

    x_data = map_data[:,0] #distance from edge (mallet channel)
    y_data = map_data[:,1] #distance along bridge (DMI)
    delamN_data = map_data[:,2] #reading from spectrogram
    delamF_data = map_data[:,3]
    time_stamp = map_data[:,4] #originally was wavespeed
    recoil_data = map_data[:,5] #bounce height
    bounce_data = map_data[:,6] #time between bounces
```

```
    return (x_data, y_data, delamN_data, delamF_data, time_stamp, recoil_data, bounce_data, time_stamp,
time_stamp)

def import_DMI(filename):
    time = []
    distance = []
    lidar_l = []
    lidar_r = []
    g = open(filename)
    for line in g:
        timeStamp = line[0:12]
        ticks = line[12:23]
        right = line[23:28] #Use these if the Lidar mount was flipped around during the scan.
        left = line[28:33]
        #left = line[23:28]
        #right = line[28:33]
        time.append(float(timeStamp))
        distance.append(float(ticks))
        lidar_l.append(float(left))
        lidar_r.append(float(right))
    g.close()
    lidarLeftRaw = lidar_l
    lidarRightRaw = lidar_r

    filterLength = 350
    #lidar_left = sp.medfilt(lidar_l,351)
    #lidar_right = sp.medfilt(lidar_r,351)

    #Pads ends of lidar arrays before filtering then truncates the filtered ends
    leftHalf1 = lidar_l[0:filterLength/2]
    leftHalf2 = lidar_l[(len(lidar_l)-filterLength/2):len(lidar_l)]
    rightHalf1 = lidar_r[0:filterLength/2]
    rightHalf2 = lidar_r[(len(lidar_r)-filterLength/2):len(lidar_r)]
    newLidarL = []
    newLidarR = []
    for x in range(len(leftHalf1)):
        newLidarL.append(leftHalf1[x])
        newLidarR.append(rightHalf1[x])
    for x in range(len(lidar_l)):
        newLidarL.append(lidar_l[x])
        newLidarR.append(lidar_r[x])
    for x in range(len(leftHalf2)):
        newLidarL.append(leftHalf2[x])
        newLidarR.append(rightHalf2[x])

    #Median Filtering
    lidar_leftFull = sp.medfilt(newLidarL,filterLength+1)
    lidar_rightFull = sp.medfilt(newLidarR,filterLength+1)
    lidar_left = lidar_leftFull[filterLength/2:(len(lidar_leftFull)-filterLength/2)]
    lidar_right = lidar_rightFull[filterLength/2:(len(lidar_rightFull)-filterLength/2)]

    return (time, distance, lidar_left, lidar_right, lidarLeftRaw, lidarRightRaw)

def combineMap(list1,list2):
    for x in range(len(list2)):
        list1.append(list2[x])
```

```
    return list1

def generateLevels(min,max,num):
    #linear
    levels = []
    for x in range(num+1):
        levels.append((max-min)*x/num+min)
    #non linear
    return levels

def make_colormap(seq):
    """Return a LinearSegmentedColormap
    seq: a sequence of floats and RGB-tuples. The floats should be increasing
    and in the interval (0,1).
    """
    seq = [(None,) * 3, 0.0] + list(seq) + [1.0, (None,) * 3]
    cdict = {'red': [], 'green': [], 'blue': []}
    for i, item in enumerate(seq):
        if isinstance(item, float):
            r1, g1, b1 = seq[i - 1]
            r2, g2, b2 = seq[i + 1]
            cdict['red'].append([item, r1, r2])
            cdict['green'].append([item, g1, g2])
            cdict['blue'].append([item, b1, b2])
    return mcolors.LinearSegmentedColormap('CustomMap', cdict)

############################Start of code upon execution#################################################
root = Tkinter.Tk()
root.withdraw()

rootDir = "../DataFiles"
file_paths = []
dmi_file_paths = []
data = []
map_data = []
dmi_data = []
xCoords = []
yCoords = []
flip = []

bridgeLength = float(raw_input("\nHow long (in feet) was the bridge?: "))
bridgeWidth = float(raw_input("How wide (in feet) was the bridge?: "))
shoulders = float(raw_input("How wide (in feet) were the shoulders?: "))

mapCount = int(raw_input("How many scans do you want to plot together?: "))
for x in range(mapCount):
    file_paths.append(tkFileDialog.askopenfilename(parent=root,initialdir=rootDir,title='Please select an \'Analysis\'
file'))
    if file_paths[x] == '': exit()
    print "\nFile ",x+1,": ", file_paths[x]
    curFilePath = file_paths[x]

    #Get file path for associated DMI file
    for y in range(len(curFilePath)):
        if (curFilePath[len(curFilePath)-y-1] == '/'):
            new_file_path = curFilePath[0:len(curFilePath)-y]
```

```
            break
    dmi_file_paths.append(new_file_path + 'DMI_File.txt')
    #print dmi_file_path

    # import the map into the variable 'data'
    data.append(import_map(curFilePath))
    #print 'Map Size:',np.size(data)

    # copy 'data' to 'map_data,' but change the data type to np.array (data is a 'tuple' and map_data is an 'np.array')
    map_data.append(np.empty([11, len(data[x][0])])) #Don't make bigger than 11, for some reason this breaks things
    for z in range(len(data[x])):
        map_data[x][z] = data[x][z]

    # import the dmi file into the variable 'dmi_data'
    dmi_data.append(import_DMI(dmi_file_paths[x]))
    #print 'DMI Size:',np.size(dmi_data)
    xCoords.append(float(raw_input("Enter X coordinate of bottom left corner of scan (x in DMI ticks): ")))
    yCoords.append(float(raw_input("Enter Y coordinate of bottom left corner of scan (mallet 7 distance in feet from
nearest parapet wall): ")))
    flip.append(raw_input("Does this scan need to be flipped (y or n)?: "))

#Putting Lidar Measurement for corresponding timestamps into map_data matrix from dmi_data
for x in range(mapCount):
    for y in range(len(map_data[x][4])):
        for z in range(len(dmi_data[x][0])):
            if map_data[x][4][y] == dmi_data[x][0][z]:
                map_data[x][7][y] = dmi_data[x][2][z]
                map_data[x][8][y] = dmi_data[x][3][z]
                map_data[x][9][y] = dmi_data[x][4][z]

#Saving Mallet# For Each Impact
for x in range(mapCount):
    for z in range(len(map_data[x][1])):
        if float(map_data[x][1][z]) == float(0): map_data[x][10][z] = float(7)
        elif float(map_data[x][1][z]) == float(2): map_data[x][10][z] = float(6)
        elif float(map_data[x][1][z]) == float(4): map_data[x][10][z] = float(5)
        elif float(map_data[x][1][z]) == float(6): map_data[x][10][z] = float(4)
        elif float(map_data[x][1][z]) == float(8): map_data[x][10][z] = float(3)
        elif float(map_data[x][1][z]) == float(10): map_data[x][10][z] = float(2)
        elif float(map_data[x][1][z]) == float(12): map_data[x][10][z] = float(1)
        else: map_data[x][10][z] = float(0)

#Adjusts x and y positions for plotting of each sample either with Lidar or fixed y distance
plotLidar = raw_input("\nDo you want to plot using the Lidar (y or n)?: ")
if plotLidar == "y":
    lidarRatio = .393 #Multiply this by the Lidar measurement to get from cm to inches
    for x in range(mapCount):
        plt.figure('Lidar Map',figsize=[20,12])
        totalPlots = 1
        pltCnt = 1
        plt.subplot(totalPlots,1,pltCnt)
        plt.title("Lidar Scan")
        plt.hold(True)
        plt.scatter(map_data[x][0],map_data[x][7],color='blue') #Left Lidar
        plt.scatter(map_data[x][0],map_data[x][8],color='green') #Right Lidar
        bluePatch = mpatches.Patch(color='blue', label='Left Lidar')
```

```
        greenPatch = mpatches.Patch(color='green',label='Right Lidar')
        plt.legend(handles = [bluePatch,greenPatch])
        plt.tight_layout()
        plt.show(block=False)
        whichLidar = raw_input("Do you want to use the left or right lidar for plotting this scan (l or r)?: ")
        #Right Lidar is about 3 inches to the left of mallet 4. Meaning it is about 21 inches to the right of Mallet 3.
        #The Lidar units are about 3 inches apart from each other so Left Lidar is 18 inches to the right of Mallet 3
        #and 6 inches to the left of Mallet 4
        if whichLidar == "l":
            for z in range(len(map_data[x][1])):
                if float(map_data[x][1][z]) == float(0): map_data[x][1][z] = float(bridgeWidth -
(lidarRatio*map_data[x][7][z] + 78)/12) #Converts each left lidar measurement to feet for each mallet
                elif float(map_data[x][1][z]) == float(2): map_data[x][1][z] = float(bridgeWidth -
(lidarRatio*map_data[x][7][z] + 54)/12)
                elif float(map_data[x][1][z]) == float(4): map_data[x][1][z] = float(bridgeWidth -
(lidarRatio*map_data[x][7][z] + 30)/12)
                elif float(map_data[x][1][z]) == float(6): map_data[x][1][z] = float(bridgeWidth -
(lidarRatio*map_data[x][7][z] + 6)/12)
                elif float(map_data[x][1][z]) == float(8): map_data[x][1][z] = float(bridgeWidth -
(lidarRatio*map_data[x][7][z] - 18)/12)
                elif float(map_data[x][1][z]) == float(10): map_data[x][1][z] = float(bridgeWidth -
(lidarRatio*map_data[x][7][z] - 42)/12) #Mallet 2 is originally indicated by a y axis value of 10
                elif float(map_data[x][1][z]) == float(12): map_data[x][1][z] = float(bridgeWidth -
(lidarRatio*map_data[x][7][z] - 66)/12) #Mallet 1 is originally indicated by a y axis value of 12
                else: map_data[x][1] = [y1+yCoords[x] for y1 in map_data[x][1]]
        elif whichLidar == "r":
            for z1 in range(len(map_data[x][1])):
                if float(map_data[x][1][z1]) == float(0): map_data[x][1][z1] = float((lidarRatio*map_data[x][8][z1] -
75)/12) #Converts each right lidar measurement to feet for each mallet
                elif float(map_data[x][1][z1]) == float(2): map_data[x][1][z1] = float((lidarRatio*map_data[x][8][z1] -
51)/12)
                elif float(map_data[x][1][z1]) == float(4): map_data[x][1][z1] = float((lidarRatio*map_data[x][8][z1] -
27)/12)
                elif float(map_data[x][1][z1]) == float(6): map_data[x][1][z1] = float((lidarRatio*map_data[x][8][z1] -
3)/12)
                elif float(map_data[x][1][z1]) == float(8): map_data[x][1][z1] = float((lidarRatio*map_data[x][8][z1] +
21)/12)
                elif float(map_data[x][1][z1]) == float(10): map_data[x][1][z1] = float((lidarRatio*map_data[x][8][z1] +
45)/12) #Mallet 2 is originally indicated by a y axis value of 10
                elif float(map_data[x][1][z1]) == float(12): map_data[x][1][z1] = float((lidarRatio*map_data[x][8][z1] +
69)/12) #Mallet 1 is originally indicated by a y axis value of 12
                else: map_data[x][1] = [y2+yCoords[x] for y2 in map_data[x][1]]
        else: map_data[x][1] = [y+yCoords[x] for y in map_data[x][1]]
        plt.close('all')

else:
    for x in range(mapCount):
        map_data[x][1] = [y+yCoords[x] for y in map_data[x][1]]

#Adds starting coordinates for each scan position on the bridge
for x in range(mapCount):
    map_data[x][0] = [y+xCoords[x] for y in map_data[x][0]]

#Flip data for scans that need it
for x in range(mapCount):
    if flip[x] == 'y':
```

```
        map_data[x][1] = [bridgeWidth-a for a in map_data[x][1]]
        maxX = max(map_data[x][0])
        map_data[x][0] = -1*map_data[x][0]
        map_data[x][0] = [y+maxX for y in map_data[x][0]]

#Combining Maps
totalMap = []
totalX = []
totalY = []
totalDelamRatio = []
totalDelam = []
totalTime = []
totalRecoil = []
totalBounce = []
totalLidarLeft = []
totalLidarRight = []
totalMalletNumber = []

for x in range(mapCount):
    totalX = combineMap(totalX,map_data[x][0])
for x in range(mapCount):
    totalY = combineMap(totalY,map_data[x][1])
for x in range(mapCount):
    totalDelamRatio = combineMap(totalDelamRatio,map_data[x][2])
for x in range(mapCount):
    totalDelam = combineMap(totalDelam,map_data[x][3])
for x in range(mapCount):
    totalTime = combineMap(totalTime,map_data[x][4])
for x in range(mapCount):
    totalRecoil = combineMap(totalRecoil,map_data[x][5])
for x in range(mapCount):
    totalBounce = combineMap(totalBounce,map_data[x][6])
for x in range(mapCount):
    totalLidarLeft = combineMap(totalLidarLeft,map_data[x][7])
for x in range(mapCount):
    totalLidarRight = combineMap(totalLidarRight,map_data[x][8])
for x in range(mapCount):
    totalMalletNumber = combineMap(totalMalletNumber,map_data[x][10])

totalMap.append(totalX)
totalMap.append(totalY)
totalMap.append(totalDelamRatio)
totalMap.append(totalDelam)
totalMap.append(totalTime)
totalMap.append(totalRecoil)
totalMap.append(totalBounce)
totalMap.append(totalLidarLeft)
totalMap.append(totalLidarRight)
totalMap.append(totalMalletNumber)

'''
#Scales Axis to user entered Bridge Length
curMax = max(totalMap[0])
for z1 in range(len(totalMap[0])):
    totalMap[0][z1] = (totalMap[0][z1]/curMax)*bridgeLength
'''
```

```
#Scales Axis to DMI measured Bridge Length --- 3583 DMI ticks = 1 foot
for z1 in range(len(totalMap[0])):
   totalMap[0][z1] = (totalMap[0][z1]/3583)
bridgeLength = max(totalMap[0])

writeFile = raw_input("Do you want to write a total map file for this bridge (y or n)?: ")
if writeFile == 'y':
   mapfile = open(rootDir +'/mapfile' + '.txt','w')
   for index1 in range(len(totalMap[0])):
      mapfile.write("{0:f} {1:f} {2:f} {3:f} {4:f} {5:f} {6:f}\r".format(totalMap[0][index1], totalMap[1][index1],
totalMap[3][index1], totalMap[4][index1], totalMap[7][index1], totalMap[8][index1], totalMap[9][index1]))
   mapfile.close()

#Finds Max and Min Delam, Mallet, and Timestamp values of Map
indexMax, valueMax = max(enumerate(totalMap[3]), key=operator.itemgetter(1))
indexMin, valueMin = min(enumerate(totalMap[3]), key=operator.itemgetter(1))
print "\nMap Max Value and Index: ", valueMax, ", ", indexMax
print "Mallet of Max Value: ", 8-((totalMap[1][indexMax]-yCoords[0])/2 + 1)
print "Max TimeStamp: ", totalMap[4][indexMax]

print "\nMap Min Value and Index: ", valueMin, ", ", indexMin
print "Mallet of Min Value: ", 8-((totalMap[1][indexMin]-yCoords[0])/2 + 1)
print "Min TimeStamp: ", totalMap[4][indexMin]
print "\n"

xList = totalMap[0]
yList = totalMap[1]

# create a uniform grid of x and y points
i = 0
xi = np.linspace(min(totalMap[0]), max(totalMap[0]), 5000)
yi = np.linspace(min(totalMap[1]), max(totalMap[1]), 1000)

#create a uniform 3D graph for each of the indicators: delam index, wave speed, recoil height, and bounce time
interpolation = 'linear'
zi_delamRatio = griddata(xList, yList, totalMap[2], xi, yi, interp=interpolation)
zi_delamF = griddata(xList, yList, totalMap[3], xi, yi, interp=interpolation)
zi_recoil = griddata(xList, yList, totalMap[5], xi, yi, interp=interpolation)
zi_bounce = griddata(xList, yList, totalMap[6], xi, yi, interp=interpolation)

'''
#******************************** Plot the 3D graphs ************************************
map_color = plt.cm.jet
map_color_r = plt.cm.jet_r
plt.figure('Bridge Maps',figsize=[20,12])
totalPlots = 2
pltCnt = 1

#Delam Raw
plt.subplot(totalPlots,1,pltCnt)
plt.title('Delamination Map')
cbar_title = 'Delamination Map'
v = np.arange(0, 700000, 10000)
CS_delam = plt.contourf(xi, yi, zi_delamF, v, cmap=map_color) #vmin = 0, vmax = 700000
plt.hold(True)
#plt.scatter(xList,yList, marker='o', c='b', s=2, zorder=10)
```

```
plt.colorbar(CS_delam)
plt.xlim(-bridgeLength/50,bridgeLength + bridgeLength/50)
plt.ylim(-bridgeWidth/10,bridgeWidth + bridgeWidth/10)
plt.plot([0,bridgeLength],[0,0],'k-',lw=3)
plt.plot([0,bridgeLength],[bridgeWidth,bridgeWidth],'k-',lw=3)
plt.xlabel('Bridge Length (ft)')
plt.ylabel('Bridge Width (ft)')
pltCnt += 1
'''

'''
#Delam Ratio
plt.subplot(totalPlots,2,pltCnt)
plt.title('Delam Ratio Map')
cbar_title = 'Delam Ratio Map'
w = np.linspace(0, 2, 3, endpoint = True)
CS_delamRatio = plt.contourf(xi, yi, zi_delamRatio, w, cmap=map_color) #vmin = 0, vmax = 700000
plt.hold(True)
#plt.scatter(xList,yList, marker='o', c='b', s=2, zorder=10)
plt.colorbar(CS_delamRatio)
plt.xlim(-bridgeLength/50,bridgeLength + bridgeLength/50)
plt.ylim(-bridgeWidth/10,bridgeWidth + bridgeWidth/10)
plt.plot([0,bridgeLength],[0,0],'k-',lw=3)
plt.plot([0,bridgeLength],[bridgeWidth,bridgeWidth],'k-',lw=3)
plt.xlabel('Sample Distance (ft)')
plt.ylabel('Mallet Number (ft)')
pltCnt += 1
'''
'''
#Recoil Height
plt.subplot(totalPlots,1,pltCnt)
plt.title('Recoil Height')
cbar_title = 'Recoil Height'
CS_recoil = plt.contourf(xi,yi,zi_recoil, generateLevels(0,130,50), cmap=map_color_r)
plt.hold(True)
plt.scatter(xList,yList, marker='o', c='b', s=2, zorder=10)
plt.colorbar(CS_recoil)
plt.xlabel('Sample Distance (ft)')
plt.ylabel('Mallet Number (ft)')
pltCnt += 1
'''
'''
#Bounce Time
plt.subplot(totalPlots,1,pltCnt)
plt.title('Bounce Time')
cbar_title = 'Bounce Map'
CS_bounce = plt.contourf(xi, yi, zi_bounce, 50, cmap=map_color_r)
#CS_bounce = plt.contourf(xi, yi, zi_bounce, generateLevels(0,0.136,50), cmap=map_color_r)
#CS_bounce = plt.contourf(xi, yi, zi_bounce, [0, 0.06, 0.08, 0.15], cmap=map_color_r)
plt.hold(True)
plt.scatter(xList,yList, marker='o', c='b', s=2, zorder=10)
plt.colorbar(CS_bounce)
plt.xlabel('Sample Distance (in)')
plt.ylabel('Mallet Number (ft)')
pltCnt += 1
'''
```

```
#plt.tight_layout()
#plt.show(block=False)

scatterPlot = raw_input("Do you want to plot with the scatter plot of impact locations (enter s)?: ")
if scatterPlot == "s":
    plt.close('all')
    plt.figure('Bridge Maps',figsize=[20,12])
    totalPlots = 1
    pltCnt = 1
    plt.subplot(totalPlots,1,pltCnt)
    plt.title('Delam Map')
    cbar_title = 'Delam Map'
    v = np.arange(0, 700000, 10000)
    CS_delam = plt.contourf(xi, yi, zi_delamF, v, cmap=map_color) #vmin = 0, vmax = 700000
    plt.hold(True)
    plt.scatter(xList,yList, marker='o', c='b', s=2, zorder=10)
    plt.colorbar(CS_delam)
    plt.xlim(-bridgeLength/50,bridgeLength + bridgeLength/50)
    plt.ylim(-bridgeWidth/10,bridgeWidth + bridgeWidth/10)
    plt.plot([0,bridgeLength],[0,0],'k-',lw=3)
    plt.plot([0,bridgeLength],[bridgeWidth,bridgeWidth],'k-',lw=3)
    plt.xlabel('Sample Distance (ft)')
    plt.ylabel('Mallet Number (ft)')
    plt.tight_layout()
    plt.show(block=False)

thresholding = raw_input("Do you want to adjust plotting thresholds (y or n)?: ")
while thresholding == "y":
    plt.close('all')
    plt.figure('Bridge Maps',figsize=[20,12])
    totalPlots = 2
    pltCnt = 1
    plt.subplot(totalPlots,1,pltCnt)
    plt.title('Delamination Map')
    cbar_title = 'Delamination Map'
    low = float(raw_input("Enter 'not delaminated' max threshold: "))
    medium = float(raw_input("Enter 'maybe delaminated' max threshold: "))
    vmax = 700000
    c = mcolors.ColorConverter().to_rgb
    #rvb = make_colormap([c('blue'), c('yellow'), low,  c('yellow'), medium, c('yellow'), c('red')]) #Faded Color Map
    rvb = make_colormap([c('blue'),low/vmax, c('yellow'),medium/vmax, c('red')]) #Blocked Color Map
    v = np.arange(0, vmax, 10000)
    CS_delam = plt.contourf(xi, yi, zi_delamF, v, cmap=rvb) #vmin = 0, vmax = 700000
    plt.hold(True)
    plt.colorbar(CS_delam)
    plt.xlim(-bridgeLength/50,bridgeLength + bridgeLength/50)
    plt.ylim(-bridgeWidth/10,bridgeWidth + bridgeWidth/10)
    plt.plot([0,bridgeLength],[0,0],'k-',lw=3)
    plt.plot([0,bridgeLength],[bridgeWidth,bridgeWidth],'k-',lw=3)
    #plt.scatter(xList,yList, marker='o', c='b', s=4, zorder=10)
    plt.plot([22,28],[0,bridgeWidth],'k-',lw=3) #Approach Span joint lines for F540
    plt.plot([bridgeLength-30,bridgeLength-24],[0,bridgeWidth],'k-',lw=3) #Approach Span joint lines for F540
    #plt.plot([20,65],[bridgeWidth,0],'k-',lw=3) #Approach Span joint lines for F463
    #plt.plot([bridgeLength-55,bridgeLength-15],[bridgeWidth,0],'k-',lw=3) #Approach Span joint lines for F463
    plt.xlabel('Bridge Length (ft)')
```

```
plt.ylabel('Bridge Width (ft)')
plt.tight_layout()
plt.show(block=False)
thresholding = raw_input("Do you want to adjust plotting thresholds (y or n)?: ")
```